Chemical Engineering Journal 471 (2023) 144400

Contents lists available at ScienceDirect

Chemical Engineering Journal

journal homepage: www.elsevier.com/locate/cej

Review

Mitigating metal-organic framework (MOF) toxicity for biomedical applications

Paulina Wiśniewska [a,b], Józef Haponiuk [a], Mohammad Reza Saeb [a,b], Navid Rabiee [c,d,*], Sidi A. Bencherif [e,f,g,*]

[a] Department of Polymer Technology, Faculty of Chemistry, Gdańsk University of Technology, Gabriela Narutowicza 11/12, 80-233 Gdańsk, Poland
[b] Advanced Materials Center, Gdańsk University of Technology, 80-233 Gdańsk, Poland
[c] Centre for Molecular Medicine and Innovative Therapeutics, Murdoch University, Perth, Western Australia 6150 Australia
[d] School of Engineering, Macquarie University, Sydney, New South Wales 2109 Australia
[e] Chemical Engineering Department, Northeastern University, Boston, MA 02155, USA
[f] Department of Bioengineering, Northeastern University, Boston, MA 02155, USA
[g] Harvard John A. Paulson School of Engineering and Applied Sciences, Harvard University, Cambridge, MA 02155, USA

ARTICLE INFO

Keywords:
Metal–organic
Framework
Toxicity
Biocompatibility
Nanoparticles
Biomedical applications

ABSTRACT

Metal-organic frameworks (MOFs) are a novel class of crystalline porous materials, consisting of metal ions and organic linkers. These hybrid materials are highly porous and have a large specific surface area, making them of great interest for applications in gas separation, energy storage, biomedical imaging, and drug delivery. As MOFs are being explored for biomedical applications, it is essential to comprehensively assess their toxicity. Although nearly ninety thousand MOFs have been investigated, evaluating and optimizing their physico-chemical properties in relevant biological systems remain critical for their clinical translation. In this review article, we first provide a brief classification of MOFs based on their chemical structures. We then conduct a comprehensive evaluation of *in vitro* and *in vivo* studies that assess the biocompatibility of MOFs. Additionally, we discuss various approaches to mitigate the critical factors associated with MOF toxicity. To this end, the effects of chemistry, particle size, morphology, and particle aggregation are examined. To better understand MOFs' potential toxicity to living organisms, we also delve into the toxicity mechanisms of nanoparticles (NPs). Furthermore, we introduce and evaluate strategies such as surface modification to reduce the inherent toxicity of MOFs. Finally, we discuss current challenges, the path to clinical trials, and new research directions.

1. Introduction

Metal–organic frameworks (MOFs) are a new class of hybrid materials consisting of metal ions linked by polymer ligands to create multidimensional structures ranging from nanometric to micrometric sizes. The combination of carefully selected inorganic and organic components yields intriguing properties not found in other solid materials. The magnificence of MOFs lies particularly in their ultra-high porosity and specific surface area, superior to traditional porous materials such as carbons or zeolites. It is reported that the surface area can reach up to 10,000 $m^2.g^{-1}$ [1] and the pores can occupy nearly 90% of the volume of the material [2]. Since MOFs are composed of exclusively strong C-C, C-O, C-H, M-O covalent bonds, they exhibit high thermal stability in the range of 250–500℃ [1]. All these features make MOFs ideal candidates for storage, capture, and/or delivery applications [3,4]. A particular potential of these structures has been recognized in the storage of gases such as hydrogen or methane, carbon dioxide capture, energy conversion and storage, as well as catalysis [1,5]. Biomedical applications, including biomedical imaging or drug delivery, are also gaining increasing attention, especially when nanoscale MOFs come to the scene. The above-mentioned potential applications (Fig. 1) are believed to be one of the main driving forces behind the development of MOFs, which over the years have become one of the most high-profile achievements in the field of chemistry, material science and nanotechnology.

The origins of research on MOFs date back to the 1960s [6]. However, it is believed that Omar Yaghi have pioneered the development of MOFs with the discovery of MOF-5 with a then record-high porosity in

* Corresponding authors.
E-mail addresses: navid.rabiee@mq.edu.au (N. Rabiee), s.bencherif@northeastern.edu (S.A. Bencherif).

https://doi.org/10.1016/j.cej.2023.144400
Received 7 April 2023; Received in revised form 22 June 2023; Accepted 24 June 2023
Available online 25 June 2023

the 1990s [7]. Its emergence has garnered much interest in the field, leading to widespread applications of MOFs. Fig. 2 gives a brief overview of the scientific progress made in the development of MOFs over the past two decades. The overall number of publications has been steadily growing from 8 in 2000 to 6,705 in 2021 with an average of 40% increase/year. Only in 2022, it has shown some stabilization, but still at a very high level (6,532 publications/year).

In addition to infinite combination possible for metal units and organic linkers and high flexibility in the design of the structural features such as geometry or pore size, there are unlimited prospects for creating MOFs. As a result, this led to the fabrication and characterization of thousands of structures each year. Out of 500,000 hierarchical MOF structures that have been predicted, it is estimated that over 90,000 MOFs have been synthesized so far [8]. Although the field of MOFs seems well advanced, there are still many aspects to consider and explore.

According to the current state of knowledge, there are some reasonable concerns regarding the safety of MOFs in biological systems. As known, all materials intended for contact with the human body must meet several restrictive requirements before being implemented. In addition to performing a specific function (having an appropriately selected structure and properties), they must be considered for their stability, biodegradability, as well as biocompatibility. The first step in assessing the toxicity of materials on living organisms is to conduct *in vitro* and *in vivo* studies. Each test provides complementary information; therefore, it is necessary to perform both. *In vitro* studies enable the precise examination of cytotoxic effect on specific mammalian cells (e.g., target-organ cells) without ethical concerns [9]. They may be especially useful in determining a possible toxicity mechanism. On the other hand, *in vivo* studies reveal the absorption and distribution of the introduced substances and their behavior throughout the organism, which gives a more extensive view than the concentration on single cells. Moreover, it also facilitates detection of previously unforeseen side effects and, consequently, the assessment of potential risk [10]. Therefore, despite promising prognosis, the use of MOFs in biomedicine will not move forward until comprehensive toxicity studies have been carried out.

So far, there have been several reports that MOFs can interact with living cells and/or tissues causing damage to them, while others declare their safety. On the other hand, several studies have hypothesized that the level of toxicity might be influenced by the physicochemical characteristics of MOFs [5,11]. Therefore, based on the above discussions, we analyze, interpret, and clarify data on the toxicity of different MOFs, focusing on precisely selected critical factors. Both *in vitro* and *in vivo* studies are discussed in detail. To the best of our knowledge, despite the high degree of interest in this field, there is a lack of a comprehensive review that systematizes the knowledge on the biocompatibility of MOFs, analyzes in depth the effect of various factors on the biosafety of these structures, and indicates a future direction for clinical trials. Previous reviews on this topic either fail to consider all the currently available reports (given the rapidly growing field) or may contain misleading information. For example, unlike the review published last year [5], which provided limited support for the effects of various factors on MOF toxicity with only a few referenced papers, our review extensively analyzes and discusses more than 20 high-impact experimental works. Additionally, we consider alternative strategies to mitigate MOF toxicity and address a clinical trial pathway that has not been previously discussed. To enhance the comprehension of the topic, we

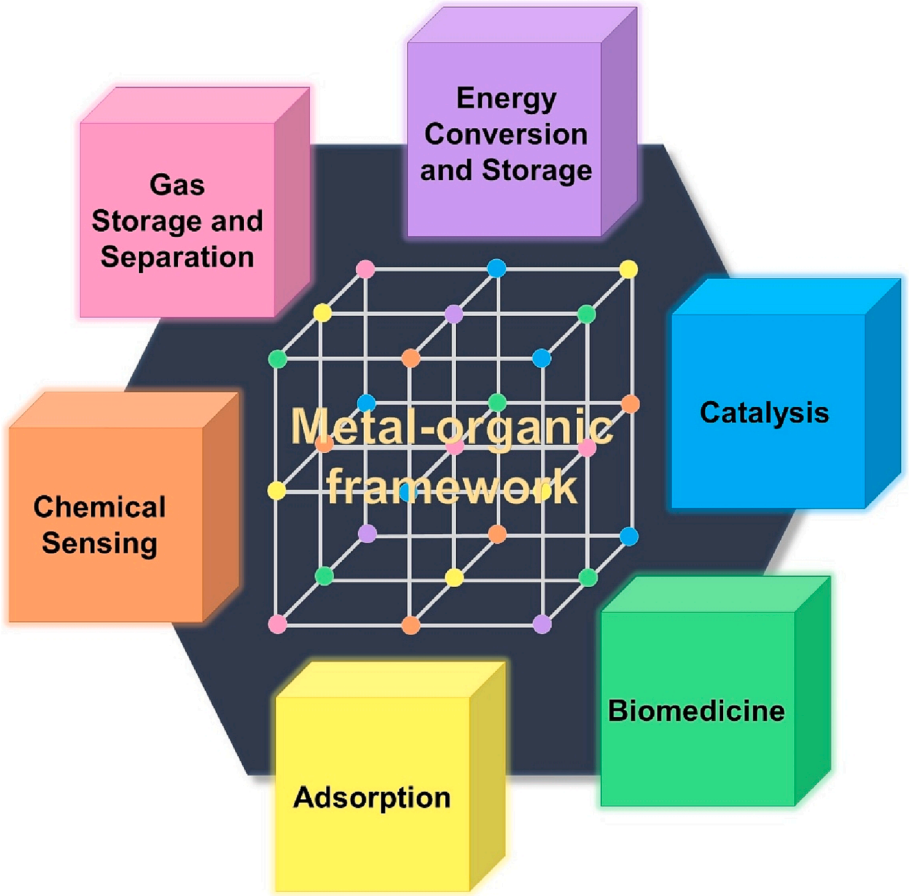

Fig. 1. *Overview of various applications of MOFs*. Application is the driving force that inspires scientists to puzzle out structural engineering. (*Designed by the authors of the present work*)

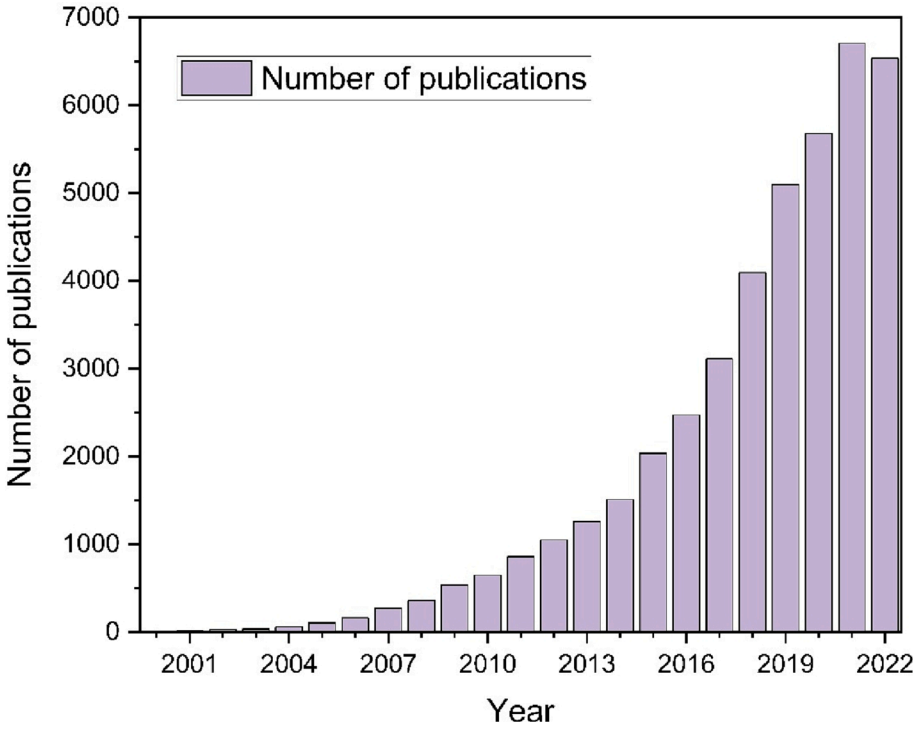

Fig. 2. *Number of published articles and reviews for MOFs (2000–2022)*. Keywords: Metal-organic framework. Source: Web of Science.

provide an explanation of the general mechanism of nanoparticle toxicity, which has not been well-defined to date.

2. MOF classification

The structural classification of MOFs provides insights into the way we think about organizing and characterizing the ever-expanding library of the synthesized MOFs. The classifications serve to facilitate exploration of structure–property relationships, discovery of new structures with desired properties, and rational design and synthesis of MOFs for specific applications. Several approaches have been proposed to classify the structural characteristics of MOFs, but there is no single and comprehensive classification of MOFs to be used for different applications. In brief, some common structural classifications that provide insights into the arrangement of metal nodes, organic linkers, and void spaces within the MOF can be named as follows:

Topological Classification: One of the most widely employed structural classifications of MOFs is based on their network topology. This classification considers the connectivity and arrangement of metal nodes and organic linkers within the framework. Topology determines the overall architecture and shape of the MOF structure and is often represented using a graph-based representation known as a net or a coordination network. Each MOF structure is assigned a unique topology based on its net, enabling systematic categorization and comparison of different MOFs. Examples of MOF topologies include the well-known MIL-53, with a diamond-shaped network [12], and UiO-66, with a Zr-based octahedral node and a linear linker [13].

Dimensionality-based Classification: MOFs can be classified based on dimensionality, which refers to the number of spatial dimensions in which the framework extends. The three common dimensionalities observed in MOFs are zero-dimensional (0D), one-dimensional (1D), and three-dimensional (3D). Zero-dimensional MOFs represent discrete clusters or isolated metal sites [14], while one-dimensional MOFs exhibit chain-like structures [15]. Three-dimensional MOFs form extended networks with porous architectures [16]. This classification provides insights into the connectivity and arrangement of metal nodes and linkers within the MOF framework.

Cage-Based Classification: Some MOFs possess large void spaces or cages within their structures. These cage-based MOFs are classified based on the shape, size, and connectivity of these void spaces. For example, cubic or octahedral cages are commonly found in zeolitic imidazolate frameworks (ZIFs) [17,18], while hexagonal prismatic and concave coordination cages are characteristic of metal–organic polyhedra (MOPs) [19] or coordination polymers (CPs). This classification highlights the unique characteristics and potential applications of MOFs with well-defined cages.

Functional Group–based Classification: Another approach to classifying MOFs is based on the types of functional groups present in the organic linkers. Organic linkers can incorporate various functional groups, such as carboxylate, pyrazolate, imidazolate, phosphonate, amine, or hydroxyl groups. The presence of different functional groups imparts specific chemical properties to the MOFs, affecting their reactivity, selectivity, and adsorption capabilities. This classification provides insights into the chemical diversity and potential applications of MOFs based on the functional groups present in their structures.

Supramolecular Classification: Supramolecular classification of MOFs focuses on the non-covalent interactions and assembly motifs within the MOF structures. This classification considers the presence of hydrogen bonding, π-π stacking, host–guest interactions, or coordination interactions between metal nodes and guest molecules. Supramolecular interactions play a crucial role in the stability, porosity, and properties of MOFs. Understanding and classifying MOFs based on their supramolecular interactions contribute to the design and control of MOF assembly at the molecular level.

It is important to note that these classifications are not mutually exclusive, and multiple criteria can be combined to provide a comprehensive understanding of MOF structures. Furthermore, advancements in computational methods, such as graph theory, machine learning, and data mining, have enabled the development of automated approaches for MOF classification, assisting in the analysis and prediction of MOF structures. However, it is not possible to provide a single classification of MOFs, due to their complex interconnected structures and wide range of varieties (some of the most used MOFs are shown in Fig. 3) [20].

Understanding the connectivity and dimensionality of the porous

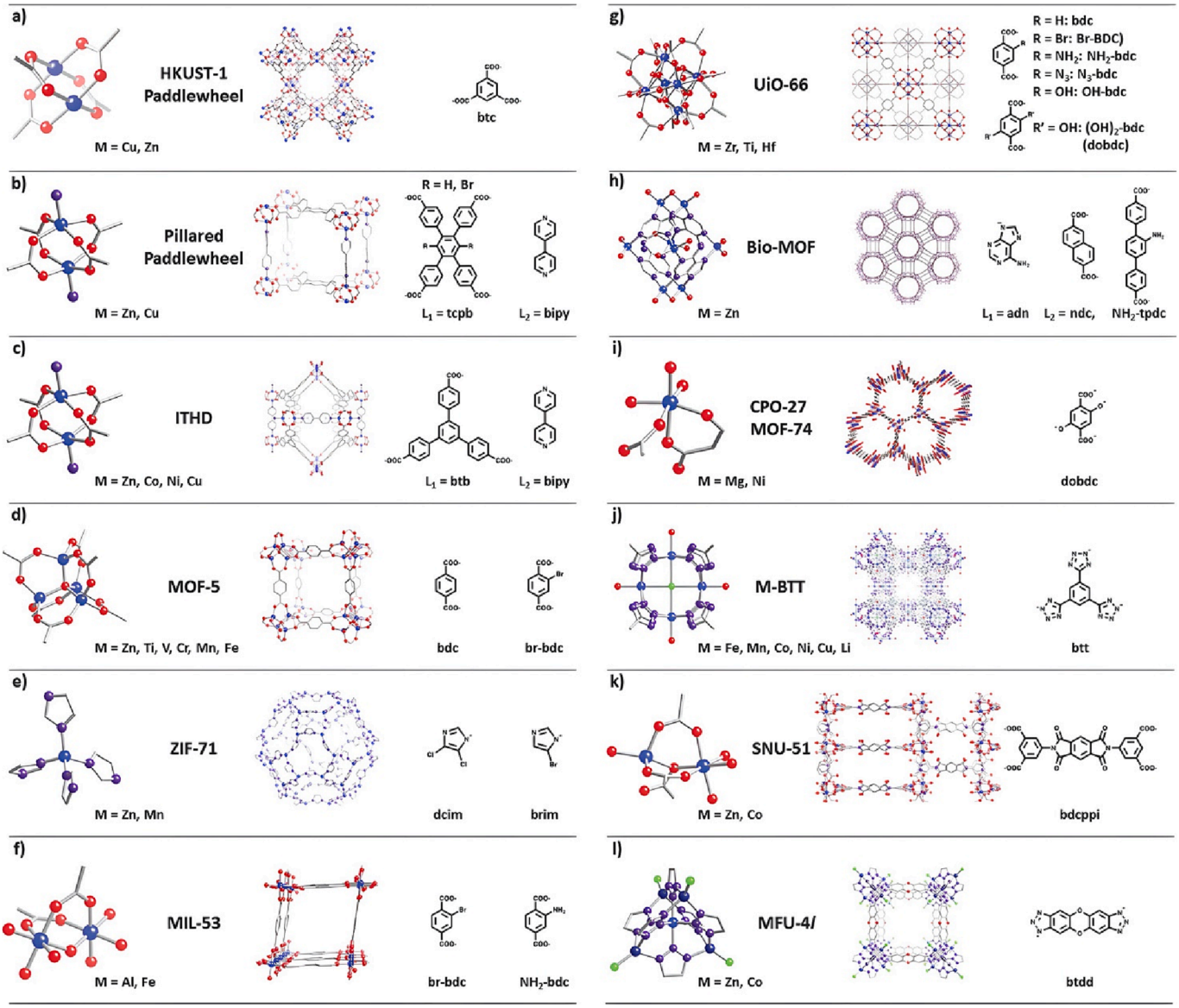

Fig. 3. *Lattice structures (middle) and corresponding Secondary Building Units (SBUs) (metal nodes (left), and organic linkers (right)) of some of the most commonly used MOFs.* Atom definition: blue – metal, red – oxygen, purple – nitrogen, grey – carbon, green – chlorine. Reproduced from Ref. [20] with permission from the Royal Society of Chemistry. (For interpretation of the references to color in this figure legend, the reader is referred to the web version of this article.)

networks in MOFs is crucial for assessing their suitability in various applications. This knowledge provides us with a different perspective to investigate the classifications of MOFs (Fig. 4a). The diverse ways in which building units are linked in MOFs lead to variations in the porous networks, where the connectivity is determined by analysing the geometric pathways connecting the porous components. These pathways give rise to different dimensional networks. Scientists analysed the accessibility and dimensionality of the pore system, by employing Poreblazer, a freely available toolkit for characterizing the structure of materials. Using Poreblazer, they examined the geometric parameters of the pore networks in a subset of 8,253 porous MOF structures. R factors for the MOF subset from 1960 to 2015 were used in this regard (Fig. 4b and Fig. 4c). The analysis revealed that 86% of the structures exhibited 1D pore connectivity, while 9% had 2D connectivity, and 4% possessed 3D connectivity, as depicted in Fig. 4a. Apart from the pore network, the dimensionality of the framework is also crucial in selecting the most suitable MOF for a specific application. While having a wide range of structures provides a comprehensive perspective on property–performance relationships, the dimensionality of the structure aids in practical decision-making. To determine the framework dimensionality, they utilized a custom script. The results encompassed 52,787 porous and non-porous MOFs. Among these structures, 40% exhibit one-dimensional (1D) dimensionality, 29% have two-dimensional (2D) dimensionality, and 31% possess three-dimensional (3D) dimensionality [21].

3. Toxicity mechanisms

The toxicity of nanoparticles (NPs) is likely due several various and distinct mechanisms. Typically, the toxic effects arise from the oxidative stress, which in turn is caused by the excess production of reactive oxygen species (ROS) such as $O_2^{\bullet-}$, $OH^{\bullet}$, $OOH^{\bullet}$. ROS can be generated by the reaction of transition metal-based NPs with H_2O_2, called the Fenton reaction as shown in Equations (1) and (2) [22]. On the other hand, ROS can also be induced by free radicals present on the reactive surface of nanoparticles. This is frequently observed after the functionalization of NPs.

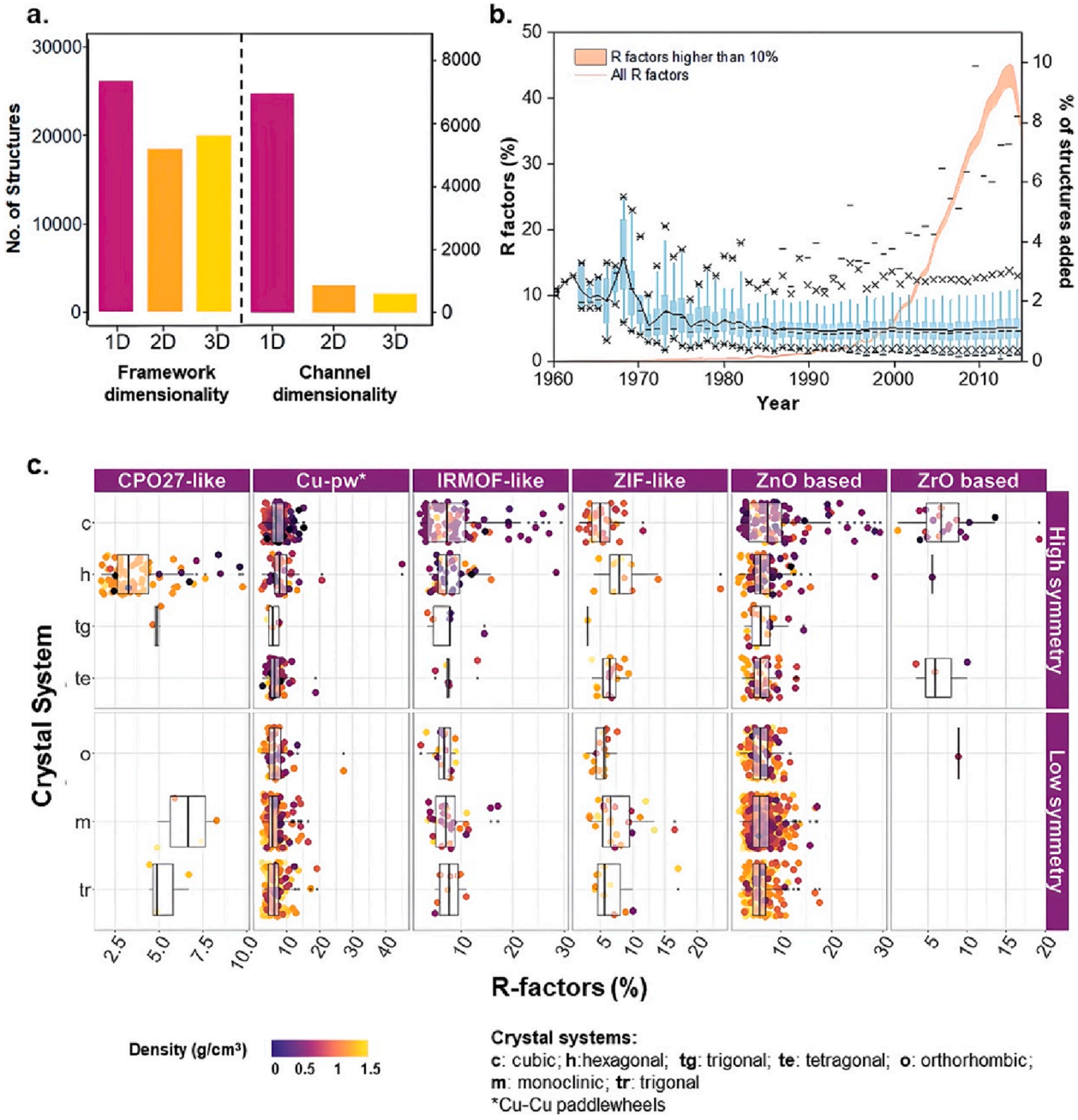

Fig. 4. *Analysis of MOFs within the Cambridge Structural Database (CSD).* (a) Histograms display the dimensionalities of frameworks and channels/pores for the dataset of 52,787 structures. (b) The non-cumulative evolution of R factors for the MOF subset from 1960 to 2015 is depicted. Boxplots in blue represent the distribution of R factors per year, with percentiles indicated by different symbols. A black line connects the means across the boxes, and the orange curve represents the percentage of structures added to the database each year. The orange area under the curve highlights the number of structures with an R factor exceeding 10%. (c) The distribution of R factors and density is presented for different MOF families and crystal systems categorized by low or high symmetry. Reproduced from Ref. [21] with permission from the Royal Society of Chemistry [12–21]. (For interpretation of the references to color in this figure legend, the reader is referred to the web version of this article.)

$$Fe^{2+} + H_2O_2 = Fe^{3+} + OH^- + OH^\bullet \quad (1)$$

$$Fe^{3+} + H_2O_2 = Fe^{2+} + H^+ + OOH^\bullet \quad (2)$$

Although a moderate level of ROS is physiologically necessary as it is involved in signal transduction or gene expression [23], their excess may lead to the damage of mitochondrial membranes but also the proteins, lipids, and mitochondrial DNA found within them. Consequently, it contributes to the activation of inflammation signaling, apoptosis or necrosis. There are several scientific papers, where such symptoms are observed in conjunction with increased level of ROS. For example, Chen *et al.* [24] observed mitochondrial membrane depolarization and the generation of apoptotic bodies in human embryonic kidney cells under the influence of copper-based MOF (HKUST-1). Simultaneously, it was estimated that at high concentration of HKUST-1, the amount of ROS was over 6 times higher compared to the control sample. Similarly, Yan *et al.* [25] found that exposure of microglia cells on cobalt-based MOF (ZIF-67) led to apoptosis by disrupting the protein signalling pathway. The generation of ROS was confirmed to be a mechanism contributing to the toxicity of ZIF-67 as the addition of the antioxidant effectively

prevented apoptosis.

The toxic behavior of NPs is also frequently attributed to the release of metal ions. This is due to the dissolution of NP in an aqueous solution and the formation of metal cations, that are indeed toxic. The toxicity of released metal ions has been repeatedly reported for ZnO and CuO NPs as Zn^{2+} and Cu^{2+} ions are particularly poisonous to living organisms. Yang *et al.* [26] confirmed that the toxicity of ZnO NPs towards NIH/3T3 cells was induced by Zn^{2+}. To prove this, they not only detected a high intracellular Zn level, but also demonstrated that very similar cell viability is achieved after exposure to Zn ions and ZnO at corresponding concentrations. A possible mechanism for the formation of Zn ions in the reaction of ZnO with CO_2 present in the cell culture environment was also proposed. Similarly, Li *et al.* [27] revealed the toxic effect of the selected MOFs on *Chlamydomonas reinhardtii* algae and attributed the release of metal ions as the mechanism responsible for their toxicity. It was found, for example, that Ni and Co based MOF (NiCo-PYZ) inhibited the *C. reinhardtii* growth by 86%. Simultaneously, the amount of nickel and cobalt ions released into algal (i.e., algae) culture medium was measured at the level of 1791 $\mu g.L^{-1}$ (87%) and 1953 $\mu g.L^{-1}$ (96%), respectively. In addition, it was shown that the appropriate amount of nickel and cobalt ions added to the algal medium instead of NiCo-PYZ resulted in comparable (88%) *C. reinhardtii* growth inhibition.

Another observed mechanism of nanoparticle toxicity is endocytosis. Endocytosis itself is one of the cellular uptakes that relies on the penetration of particles into the cell by enclosing them in vacuoles. Phagocytosis, pinocytosis, clathrin and caveolae-mediated endocytosis can be named as the main types of endocytosis. The toxicity resulting from this type of uptake is attributed to the free movement of NPs within the cells. For example, NPs introduced via pinocytosis may distribute in cell membrane, cytoplasm, lipid vesicles, mitochondria, or nucleus. Depending on the localization, they can damage DNA or organelles, and ultimately lead to cell death [28]. Eom and Choi [29] demonstrated that clathrin-mediated endocytosis is involved in silica nanoparticles uptake and causes *Caenohabditis elegans* toxicity (i.e., reduces its reproductive ability). The role of the endocytic pathway in SiNPs internalization was confirmed using specific inhibitors for various types of endocytosis. The toxic effect was found to be related to the clathrin-mediated endocytosis uptake, since reproduction was also investigated using endocytosis defective mutants. Interestingly, no increase in ROS level was observed due to the presence of SiNPs.

The toxic effect of nanoparticles may also be induced by the cell membrane damage caused by NPs adsorption on the cell surface or their diffusion. Brayner *et al.* [30] and Raghupathi *et al.* [31] suggested that ZnO nanoparticles inhibit the growth of *Escherichia coli* and *Staphylococcus aureus*, respectively, due to their accumulation in the bacterial membrane and subsequent disorganization. Ruenraroengsak *et al.* [32] also indicated membrane damage as an alternative mechanism of human alveolar type 1-like epithelial cell death upon the exposure of amine-modified NPs. Gogniat *et al.* [33] demonstrated that the adsorption rate of TiO_2 on the *Escherichia coli* cells is correlated with its bactericidal effect. Importantly, flow cytometry analysis revealed that adsorption contributed to the reduction of bacterial membrane integrity. *E. coli*

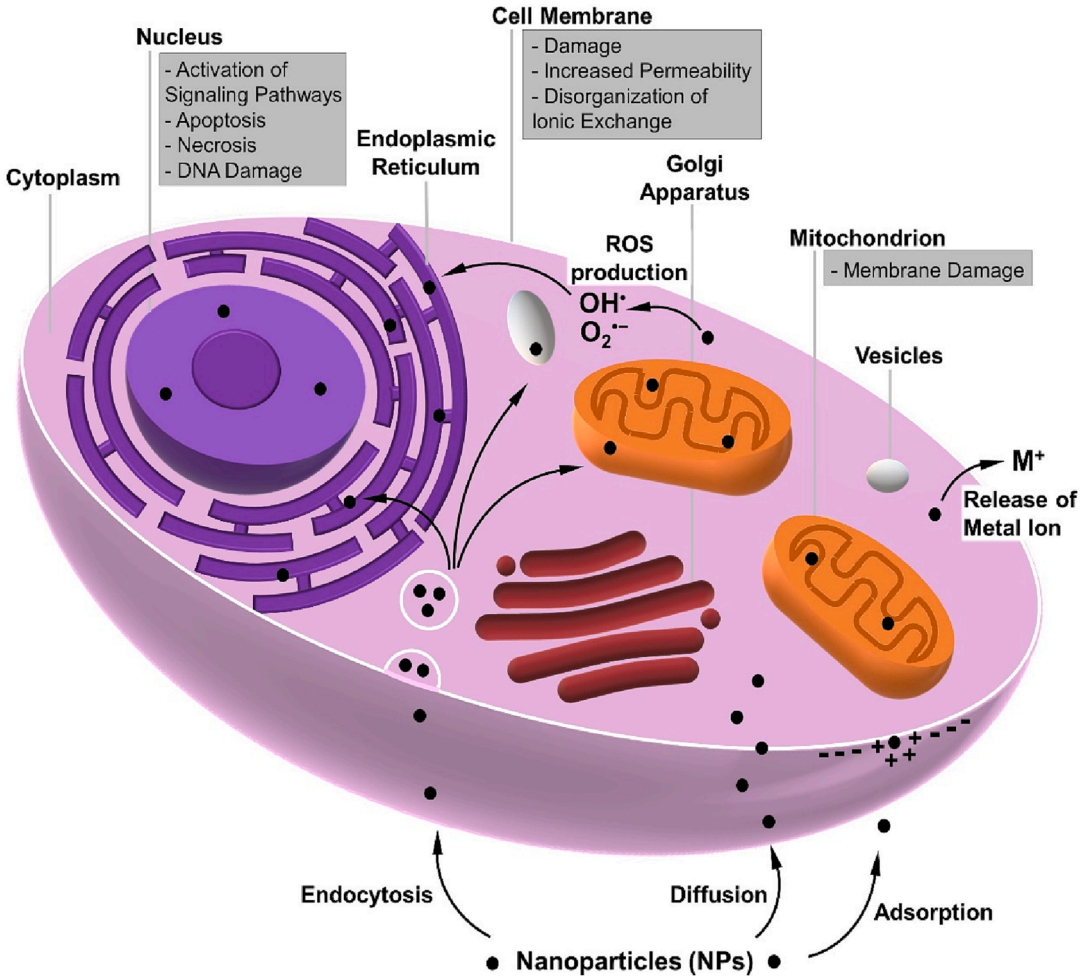

Fig. 5. *Schematic illustration of the main mechanisms associated with MOF-induced toxicity.* MOF-related toxicity can occur during the cellular internalization stage (endocytosis, diffusion, adsorption), resulting in membrane damage. Due to potential ROS production, internalized MOFs such as MOF NPs can also pose a risk to other cell structures (e.g., mitochondria, nucleus). (*Designed by the authors of the present work*)

membrane damage caused by the diffusion of nanoparticles into the cell was also observed in the TEM images presented by Stoimenov *et al.* [34].

Recently, it has been found that the toxicity of the nanoparticles may also be associated with fibrinogen unfolding. Binding of NPs to fibrinogen is known to cause physiological and pathological changes such as macrophage uptake, blood coagulation, and protein aggregation, but the mechanisms leading to these abnormalities have been poorly understood so far. The first step in this direction was taken by Deng *et al.* [35] who reported that negatively charged nanoparticles bind to fibrinogen and induce its unfolding, which consequently activates the Mac-1

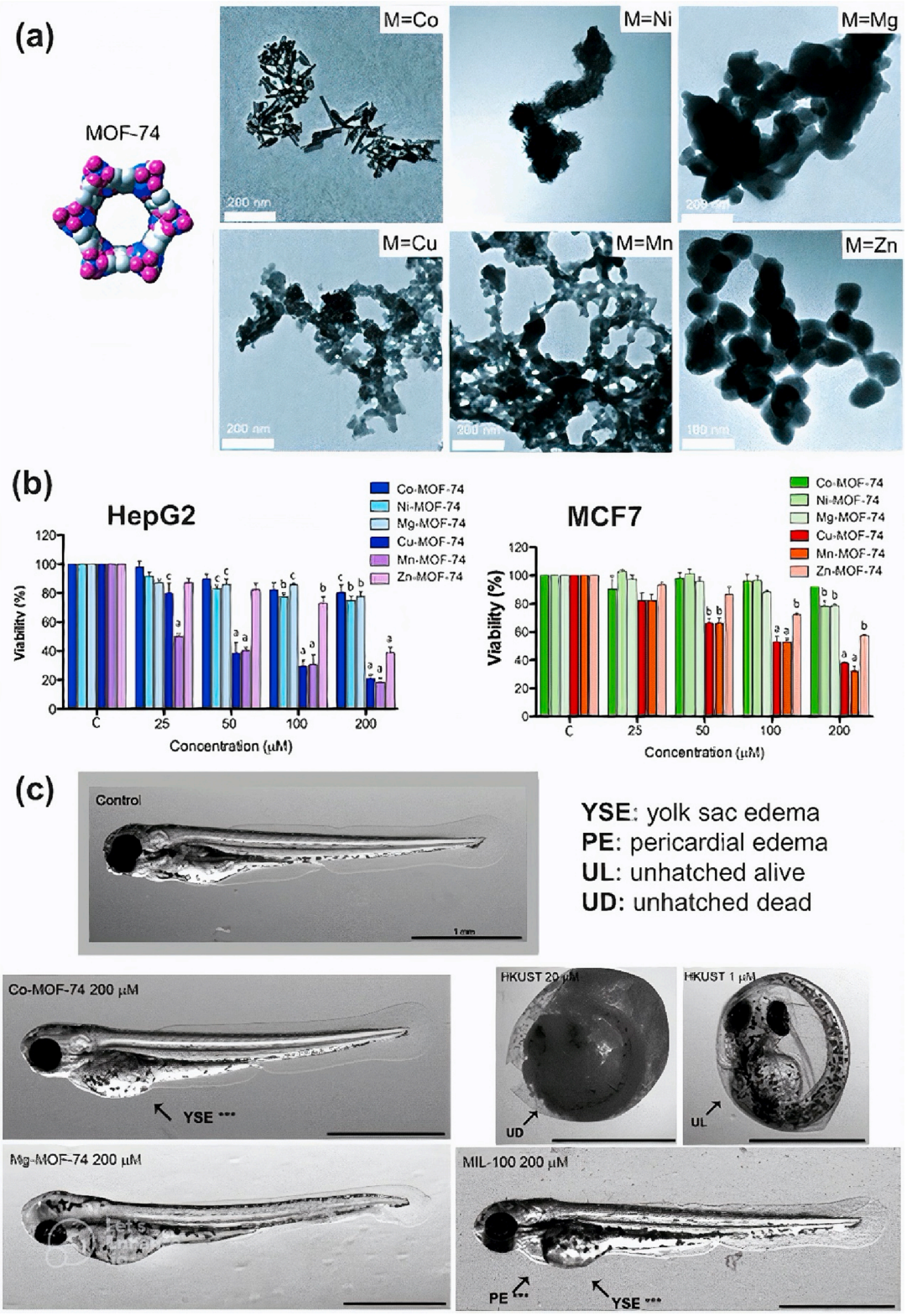

Fig. 6. *Characterization of MOF-74.* (a) TEM images of MOF structures. (b) HepG2 and MCF7 cell viability 24 h after MOF incubation. (c) Zebrafish embryos 72 h post fertilization. Reprinted with permission from [37]. Copyright 2014 John Wiley and Sons.

integrin receptor. This in turn disrupts the signalling pathway, leading to the release of inflammatory cytokines. Moreover, it was suggested that the secretion of pro-inflammatory cytokines may exacerbate inflammation in Alzheimer's disease or arthritis, but further research is needed to confirm this assumption. A simplified scheme of the most common mechanisms of NP toxicity is shown in Fig. 5. Although the mechanisms of toxicity illustrated and described above are to some extent well defined and in some cases may explain how toxicity was induced, there are still many potential mechanisms that have yet to be discovered.

4. MOF toxicity

Recent studies have shown that physico-chemical parameters are principal determinants of MOF toxicity [5,36]. In this section, we evaluate the effect of critical factors such as (*i*) chemistry of precursors, (*ii*) particle size, (*iii*) morphology, and (*iv*) zeta potential/aggregations on the inherent MOF toxicity. Both various types of MOFs and studies against different cell lines/animals are taken into considerations. In addition, all reviewed data will be used to create a comprehensive table, in which one can find the overall degree of MOF toxicity, including when subjected to physico-chemical factors.

4.1. Chemistry of precursors

Chemistry of precursors, including metal ions and organic ligands, used in the synthesis of MOF directly determines its chemical composition, which in turn largely influences its toxicity behavior. Since the precursors can be selected independently, we decided to discuss the role of metal nodes and organic linkers separately.

4.1.1. Chemistry of metals

By analysing the half maximal inhibitory concentration (IC_{50}) parameter of different MOFs (approximately 50 papers were reviewed), we found that the effect of metal often determines the overall toxicity of MOF. Despite the diversity of factors and studies conditions, we can rank the most commonly used metals in terms of MOF biosafety. Accordingly, structures containing Cu, and Mn can be classified as high toxic, with Zn, Fe, Co, and Al as medium toxic, and those composed of Cr, Zr, and Mg as low toxic. Nevertheless, to provide even more reliable conclusions, we considered several studies where the type of metal is the only variable in the examined MOFs. The reported results largely correspond to this overall ranking; however, they provide more detailed information within individual groups.

The most comprehensive study in this regard was performed by Ruyra *et al.* [37] who synthesized and examined among others a series of MOF-74 composed of the following metal ions: Zn^{II}, Cu^{II}, Ni^{II}, Co^{II}, Mn^{II}, and Mg^{II} (Fig. 6a). Based on the results of the HepG2 and MCF7 cell viability assay (Fig. 6b), it was found that Cu- and Mn-MOF-74 exhibit the highest toxicity, while Co, Ni, Mg based counterparts are biocompatible. In the case of Zn-MOF-74, a moderate level of cytotoxicity was recognized. The *in vivo* studies on selected structures revealed that zebrafish embryos exposed to Co-MOF-74 experienced yolk sac edema, contrary to embryo incubated with Mg-MOF-74 as shown in Fig. 6c. In addition, other MOFs such as MOF-5(Zn) and UiO-66(Zr), containing 1,4-benzenedicarboxylic acid as the organic part, were considered. It was noticed that the cell viability varied significantly with the injected NPs. As much as UiO-66(Zr) did not crucially affect the cell viability, the injection of 200 μM MOF-5(Zn) led to more than 80% mortality, which proves that Zn contributes to the increase of MOF toxicity. Another example of comparative MOFs were MIL-100(Fe) and HKUST-1(Cu) comprising of 1,3,5-benzenetricarboxylic acid in their structure. Based on the *in vitro* analysis, it was found that there is a certain toxicity of both NPs, but clearly higher for the Cu-based MOF. For instance, the viability of HepG2 cells after administration of 200 μM MIL-100(Fe) and HKUST-1(Cu) decreased to 53% and 17%, respectively. On the other hand, *in vivo* studies provided even more interesting results. It was shown that the hatching rate of zebrafish embryos under the influence of 1 μM HKUST-1(Cu) reached 8.3%, while all embryos incubated with 200 μM MIL-100(Fe) hatched. Nevertheless, numerous malformations were observed, such as pericardial and yolk sac edema (Fig. 6c).

Slightly different assessment of the toxicity of Co- and Zn-based MOFs was provided by Hao and Yan [38]. The scientists focused on the hematotoxicity of ZIFs due to their inevitable contact with blood in potential biomedical applications. It was reported that ZIF-67 composed of Co resulted in a significant hemolysis of red blood cell, unlike to ZIF-8 (Zn). The membrane rupture phenomenon was a consequence of the generation of superoxide anions and hydroxyl radicals, followed by hemoglobin binding. On the other hand, Zhang *et al.* [39] found certain comparable phytotoxicity of ZIF-67 and ZIF-8. For example, at a concentration of 0.1–1 $mg.L^{-1}$ algal growth inhibition (by 1–32%), chlorophyll content reduction (by 7–30%), membrane permeation or chloroplast damage was observed. However, interestingly, the results of this study confirmed that the above-mentioned parameters are recoverable as early as 72 h after the elimination of MOF, which gives a very promising prognosis, even for moderately toxic NPs.

So far, MIL-100 has been the most frequently studied structure in terms of biocompatibility [5]. Grall *et al.* [40] evaluated and compared the *in vitro* toxicity of three MIL-100 containing Fe^{III}, Al^{III}, or Cr^{III}. It was shown that none of the studied MOFs induced any toxicity in the A549, Calu-3, and HepG2 cells even at high doses (64 $\mu g.cm^{-2}$). Only slight toxicity (~39% cell mortality) was observed against Hep3B cells after exposure to 64 $\mu g.cm^{-2}$ MIL-100(Fe) which was in line with increased (1.8-fold) level of the oxidative stress. According to the authors, the induction of ROS in the presence of MIL-100(Fe) may be related either to the redox character of iron (the standard potential of Fe^{3+} is higher compared to Al^{3+} and Cr^{3+}) or ability to form hydroxyl radicals such as in the Fenton reaction (Equation (2)). In addition, considering that potential genotoxicity results from oxidative stress, the conducted research on Hep3B cells was extended to the measurement of DNA damage. This was quantified by counting the number of γ-H2Ax foci per nuclei. It was revealed that only for Fe-based MOF at a concentration of 64 $\mu g.cm^{-2}$ an increase in the median foci from 3 to 5 per nuclei was observed ($0.01 < p < 0.05$). Although the level of DNA damage seems relatively low, it must be considered that Hep3B cells lack p53 (e.g., unlike HepG2 cells) and that only one DNA double-strand break can be lethal to cell integrity.

A similar toxicity profile of the MIL-100 compounds was obtained by other researcher groups. Hidalgo *et al.* [41] demonstrated that neither MIL-100(Fe) nor MIL-100(Al) induced toxicity against the J774.A1 cells, even at high concentrations (1200 $\mu g.mL^{-1}$). Nevertheless, in both cases higher secretion of pro-inflammatory cytokines was observed. The greatest changes were noted for TNF-α level (4 ANOVA stars) produced from peripheral blood mononuclear cells in the presence of 25 $\mu g.mL^{-1}$ MIL-100(Fe) or 250 $\mu g.mL^{-1}$ MIL-100(Al). On the other hand, Wuttke *et al.* [42] found that although there were no signs of apoptotic HMEC cell death and no inflammatory response in HUVEC cells treated with MIL-100(Fe) or MIL-101(Cr), a significant decrease in MLE12 metabolic activity was observed at 100 $\mu g.mL^{-1}$ MIL-100(Fe) and 200 $\mu g.mL^{-1}$ MIL-101(Cr). In addition, Fe-based MOF showed strong inhibition of MH-S cell viability in the MTT and LDH assays as low as 25 $\mu g.mL^{-1}$, whereas Cr-MOF induced cell death only at the highest dose of 200 $\mu g.mL^{-1}$, which indicates slightly lower tolerance of human cells to MIL-100(Fe) compared to MIL-101(Cr).

Comparably low cytotoxicity of MOFs composed of Fe, Al, and Zr as well as Al and Zr was also confirmed by Duan *et al.* [43] and Sifaoui *et al.* [44], respectively. Duan *et al.* [43] showed that when tested with HDF, 3 T3, and HeLa cells, IC_{50} values ranged between 4430 and 7230 $\mu g.mL^{-1}$ for Fe-based PCN-333 and 3840–6610 $\mu g.mL^{-1}$ for Al-based PCN-333. However for MOFs composed of 1,4-benzenedicarboxylic acid, IC_{50} values ranged between 4920 and 7200 for Fe-based MOFs, 3690–6400 for Al–based MOFs, and 6400–7200 $\mu g.mL^{-1}$ for Zr-based MOFs. In addition, they showed that hemolytic rate did not exceed 2.5 % even at

high concentration of MOF, which again proves biosafety of these structures. Similarly, the IC_{50} value for CIM-80(Al) or CIM-84(Zr) against J774.A1 cells, provided by Sifaoui *et al.* [44], was above 5000 $\mu g.mL^{-1}$. Moreover, these results agreed with *in vivo* assay, which revealed that all amphipods treated with Al- and Zr-based MOF survived. Interestingly, other structures composed of Zn (CIM-81 and CIM-91), analyzed in parallel, resulted in the death of all animals.

Metal-dependent toxicity was also found by Tamames-Tabar *et al.* [45] who claimed that J774 and HeLa cells tolerated the Fe-based MOFs better than Zr and Zn. For example, IC_{50} values of MIL-88B(Fe) and UiO-66(Zr), consisting of 1,4-benzenedicarboxylic acid, were equal to 1260 and 400 $\mu g.mL^{-1}$ (HeLa cells) and 370 and 60 $\mu g.mL^{-1}$ (J774 cells),

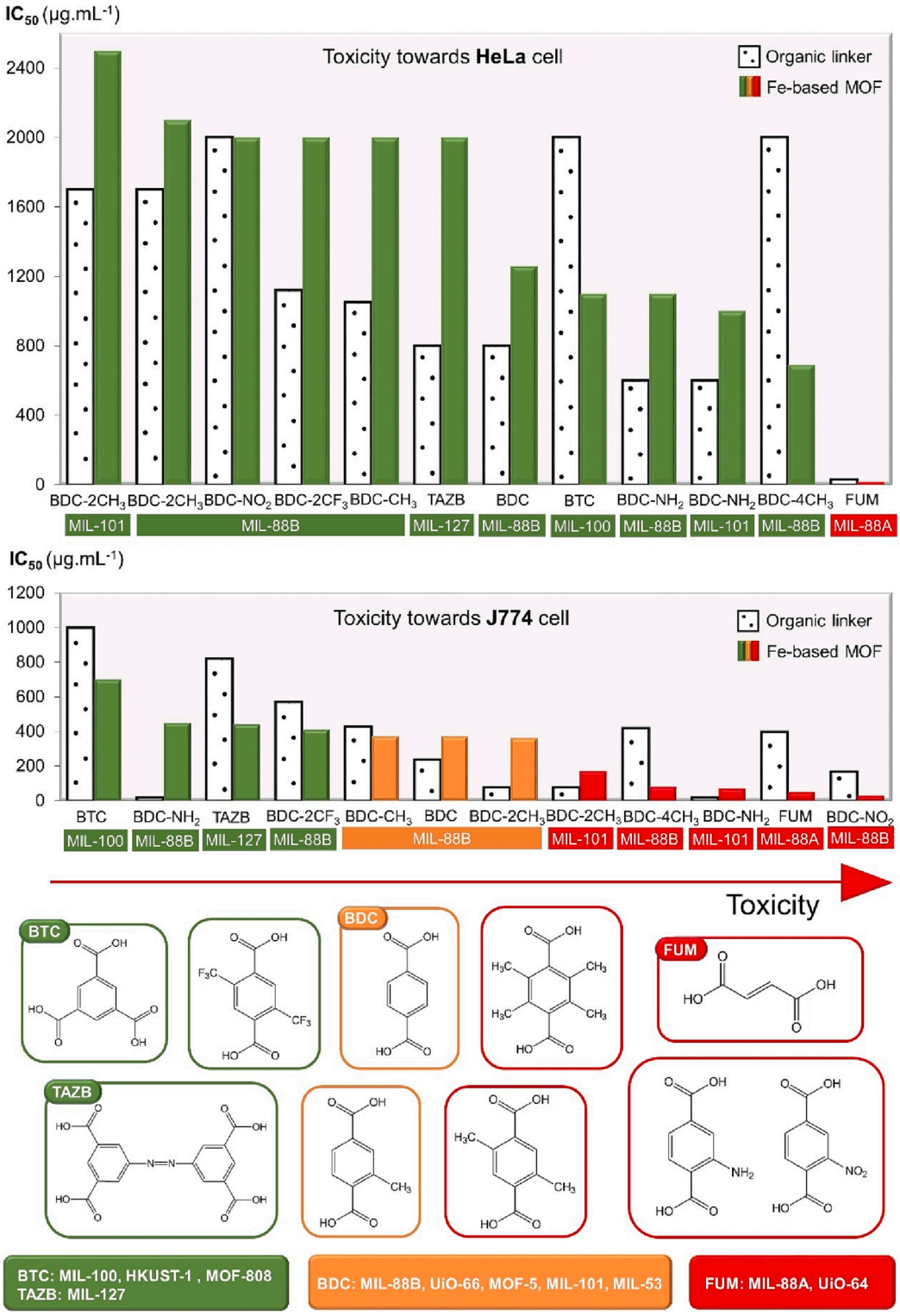

Fig. 7. *Toxicity of organic ligands and corresponding Fe-contained MOFs towards HeLa and J774 cells based on reported IC_{50} data* [45]. Chemical names of the structures - BTC: 1,3,5-benzenetricarboxylic acid, TAZB: azobenzenetetracarboxylic acid, BDC: 1,4-benzenedicarboxylic acid, and FUM: 2-butenedioic acid. (*Designed by the authors of the present work*)

respectively. Interestingly, IC_{50} values of ZIF-8(Zn) were 100 μg.mL^{-1} (HeLa cells) and 25 μg.mL^{-1} (J774 cells) despite the lower toxicity of its organic ligand. It was suggested that Zn toxicity is attributed to the high solubility of Zn^{2+} ions, while the Zr^{4+} complexes were believed to be antiproliferative. In turn, the differences in toxicity against the two cell lines were mainly attributed to the faster internalization of MOFs.

In conclusion, metal ions strongly govern MOF toxicity, which was highlighted and validated in numerous studies [37,43,45]. Therefore, to design safe MOFs for biomedical applications, the type of metals should be carefully considered.

4.1.2. Chemistry of organic linkers

Several attempts have been made to examine the effect of organic linker type on the toxicity of MOF so far. Nevertheless, understanding this relationship turns out to be quite a challenge, as the literature data provide multilateral findings. The most representative study comparing the toxicity of selected MOFs and their constituent organic parts themselves was conducted by Tammes-Tabar *et al.* [45]. Fig. 7 provides an informative toxicity assessment of several organic linkers and their corresponding Fe-contained MOFs based on the reported IC_{50} data. Interestingly, it can be noticed that the cytotoxicity to HeLa and J774 cells varied considerably as some structures were found to be cytocompatible to HeLa cells while being highly toxic to J774 cells. It is worth mentioning that the toxicity of various MOFs did not always correspond to the toxicity of their organic part itself, although the metal ion remained unchanged. In other words, the characterisation of the MOF is not a simple reflection of its precursors. Moreover, even MOFs composed of identical precursors (Fe ion and 2-amino-1,4-benzenedicarboxylic acid) was found to act differently to the J774 cell growth inhibition This is the best evidence that the toxicity is a very complex feature that depends on many factors that we have not been able to explore yet. Nevertheless, we decide to distinguish linkers such as fumaric acid, as well as some terephthalic acid derivatives (BDC-NO_2, BDC-4CH_3, BDC-NH_2), possibly responsible for the increased toxicity of MOFs. A certain trend towards toxicity (from a chemical point of view) is sketched in Fig. 7. It should be highlighted that although all examined ligands are carboxylic acids, their level of biosafety was different. Moreover, the incorporation of various functional groups into 1,4-benzenedicarboxylic acid seems to be of little benefit from the MOF biosafety point of view. Authors suggest that MOF toxicity may be determined by the hydrophilic-hydrophobic character of the organic linker, since the most toxic effect on the J774 cell was noted for hydrophobic compounds (i.e., BDC-CH_3, BDC-NO_2) with the exception of fumaric acid, while the hydrophilic 1,3,5-benzenetricarboxylic acid (BTC) was the least harmful to the J774 cell. This theory was supported by the ability of hydrophilic compounds to be easily excreted which prevents their negative impact on the biological system. In addition, other researchers [46] confirmed that only trace amounts of fumaric acid can be detected in the urine after MIL-88A accumulation, suggesting its reuse by the Krebs cycle.

Some efforts were also made to investigate the effect of different Fe-based MOFs on the *in vivo* toxicity and biodistribution [46]. It was reported that all rats survived the administration of 220 mg.kg^{-1} of MIL-100 or MIL-88A, or 110 mg.kg^{-1} MIL-88B-4CH_3. Moreover, all organs such as liver, spleen, kidney, heart, and brain kept their function intact without any signs of persistent toxicity. Only slight abnormalities in the liver color or splenic hyperplasia were observed, but all changes completely disappeared by 30 days after injection. Interestingly, it was evidenced that the content of individual organic linkers in the liver and spleen 1 day after MOFs incorporation was different. For example, approximately 37 and 8% of BDC-4CH_3 (MIL-88B-4CH_3 organic part) was detected to be distributed in the liver and spleen, respectively, but only 17 and 3% of the dose of 1,3,5-benzenetricarboxylic acid (MIL-100 organic part). It means that the chemical structure of the organic linker affects the biodistribution of MOFs, as the actual dose in individual cell/organs differs considerably.

The organic linker-dependent toxicity of MOFs was also studied by other research groups. For example, Sifaoui *et al.* [44] demonstrated that UiO-64(Zr) composed of fumaric acid (FUM) was more toxic than UiO-66(Zr) containing 1,4-benzenedicarboxylic acid (BDC), which is in agreement with the trend presented in Fig. 7. They revealed that injection of 2500 μg.mL^{-1} UiO-64 led to the death of most amphipods, while all organisms incubated with UiO-66 survived but showed reduced mobility. Interestingly, no evident *in vitro* toxicity was observed in any structure against J774.A1 cell up to 5000 μg.mL^{-1}.

Furthermore, Ruyra *et al.* [37] reported more severe toxicity to zebrafish embryos exposed to MIL-100(Fe) rather than MIL-101-NH_2(Fe), which consists of 1,3,5-benzenetricarboxylic acid (BTC) and 2-aminobenzene-1,4-dicarboxylic acid (BDC-NH_2), respectively. They showed that although both structures caused multiple morphological defects such as pericardial or yolk sac edema, only embryos treated with MIL-101-NH_2 failed to hatch. Surprisingly, *in vitro* studies indicated slightly lower HepG2 and MCF7 cell viability under the influence of MIL-100 (50–80% vs. 70–90% at 200 μM), however, the overall toxicity in both cases was moderate. In addition, the researchers also provided interesting insights with respect to other MOFs. For instance, they observed that cytotoxicity may varied significantly in terms of tested cell. UiO-66-NH_2 was not well tolerated by HepG2 cell, as it resulted in an approximately 50% decrease in their viability, while it was highly biocompatible with MCF7 cell. Consequently, comparing the toxicity of this MOF with UiO-66, which differs only in the structure of the organic linker, can lead to twofold conclusions, indicating both higher and lower toxicity. Finally, they demonstrated that ZIF-8 is much more damaging to biological systems compared to ZIF-7 based on the results of both *in vitro* and *in vivo* studies, although both contain imidazolates: benzylimidazole and 2-methylimidazole, respectively. This is another evidence that the MOF toxicity is determined by individual compounds rather than defined chemical groups such as carboxylates, amines, or imidazolates.

A significant differences in the cytotoxicity of ZIF-90 and its several modified versions, in which aldehyde groups of organic ligand were substituted with carboxyl (ZIF-90-C), amino (ZIF-90-A), or thiol (ZIF-90-T) groups without interfering the framework were also revealed by Yen *et al.* [47]. Based on the cell viability assay it was found that ZIF-90 modified with amino groups induced the highest toxicity, followed by ZIF-90-T and ZIF-90-C. The IC_{50} value of HEK-293 and MCF-7 cells was 30–37, 31–50, 52–70, and 49–72 mg.mL^{-1}, respectively, with the last value corresponding to the unmodified sample. The authors assume that this phenomenon can be explained by the fact that nZIF-90-A has a relatively positive surface potential compared to other MOFs, which leads to stronger electrostatic interactions toward cell membranes with a slightly negative charge. Consequently, this may result in either disruption of the cell membrane, or more efficient cell uptake. Nevertheless, the concentrations at which certain toxicity occurred are relatively high, so all structures may be considered for biomedical applications.

The effect of the organic linker on the toxicity of different MOFs containing the same metal node was also examined by Duan *et al.* [43]. The results of MTT assay showed that all tested Fe-, Al-, and Zr-based MOFs induced low toxicity, regardless of the structure of the organic compound (TATB ~ BDC ~ BTC, TATB ~ BDC, BTC ~ BDC) and the tested cell (HDF, 3 T3, HeLa). The IC_{50} parameter ranged from 3690 to 9600 μg.mL^{-1}. However, it is worth mentioning that the HKUST-1(Cu), composed of BTC, achieved 5–17 times lower IC_{50} value (560–1140 μg.mL^{-1}) compared to other MOFs, which proves that the metal determines the toxicity more than the organic linker. Furthermore, other toxicity studies such as hemolytic behavior or mice skin penetration assay were also conducted. The obtained results were consistent with the results obtained from the cell viability assay, confirming the good biocompatibility of MOFs. Although the hemolysis rate ranged slightly among the tested NPs, it was well below the 5% clinical safety standard. Similarly, the skin irritation test showed no abnormalities in the form of erythema, edema, or other allergic symptoms after various MOF treatment.

To sum up, the type of organic linker undoubtedly affects MOF toxicity; however, considering all the presented studies, this dependency is not straightforward. It is also worth paying attention to the fact that the toxicity of organic linker (or the MOF representing it) varied significantly in relation to the tested cells/organs even within one study. Accordingly, we conclude that although organic ligands do not determine toxicity as directly as metal ions do, they do play an important role in their selective adsorption and biodistribution.

4.2. Particle size

Ideally, the development of bio-MOFs would be the best solution to avoid toxicity. However, when it comes to application, the environment in which they are utilized plays a significant role in determining their toxicity [48]. The particle size of MOFs is one of the key factors that needs to be considered for ensuring non-toxic biomedical applications [49,50]. It was found that downsizing MOFs to the nanoscale may improve pharmacological performance, including drug delivery efficiency and controlled release [51]. On the other hand, some features of NPs such as larger surface area, higher chemical reactivity and penetration ability compared to the corresponding bulk materials may raise concerns about toxic effects on living organisms. For example, NPs are able to cross biological membranes and enter the bloodstream through inhalation or ingestion, whereas larger particles normally cannot [52]. Therefore, in this subsection, we evaluate what sizes and concentrations of various MOFs can be safely used in biological systems.

To begin with, it is of a crucial importance to compare *in vitro* and *in vivo* toxicity of nano- versus micro-dimensional MOFs. For this purpose, two recent studies were carried out, which revealed that nanoscale MOFs (n-MOF) are safer for living organisms compared to the micron-sized MOFs (m-MOF). For example, Zhu *et al.* [53] synthesized Mg-MOF74 with an average particle size of 3–4 μm (m-Mg-MOF74) and 250–350 nm (n-Mg-MOF74). Based on the MTT assay, it was proved that cytotoxicity to HeLa cells is triggered when exposed to more than 500 $\mu g.mL^{-1}$ m-Mg-MOF74 or 1000 $\mu g.mL^{-1}$n-Mg-MOF74. The value of IC_{50} parameter was estimated at 798 $\mu g.mL^{-1}$ and over 2000 $\mu g.mL^{-1}$, respectively. Moreover, n-Mg-MOF74 indicated lower apoptosis cells than m-Mg-MOF74 at 1000 $\mu g.mL^{-1}$, however, this difference was not significant at higher concentration (2000 $\mu g.mL^{-1}$). Interestingly, due to the increased bioavailability of Mg^{2+}, it was observed that n-Mg-MOF74 have better osteogenic potential compared to micron-sized MOF (e.g., it exhibited greater collagen secretion in BMSC cells at the same concentrations). On the other hand, *in vivo* studies showed slightly lower cardiotoxicity and less effect on the growth of rats under n-Mg-MOF74 than m-Mg-MOF74 treatment, however, no significant evidence of toxicity of any of them was found. This positive effect of nanoscale Mg-MOF74, authors attribute to the balanced release of Mg^{2+} both inside and outside the cells.

Similarly, lower toxicity of n-MOF compared to m-MOF was found by Jiang *et al.* [54]. The scientists synthesized and examined bio-MOF-1 with a dimension of 400–600 nm and 50–80 μm (Fig. 8a-d). Selected results of performed *in vitro* and *in vivo* toxicological analysis were collected and presented in Fig. 8e-l. For example, as shown in Fig. 8e, it can be noticed that at concentrations above 100 $\mu g.mL^{-1}$, there is a considerable variation in MC3T3-E1 cell death among micro/nano (m/n) structures (2–3 ANOVA stars). The IC_{50} value of n-bio-MOF-1, calculated as 599.3 $\mu g.mL^{-1}$, was also significantly higher than that of m-bio-MOF-1 (248.3 $\mu g.mL^{-1}$). These results are in agreement with biochemical blood tests in rats that indicated moderate level of biosafety at doses above 100 $\mu g.mL^{-1}$. Histological observation further showed that groups exposed to nanoscale MOF retained a better biocompatibility than those of micron size.

Although above studies indicated higher biocompatibility of n-MOFs compared to m-MOFs, it should be considered that the nanoscale is a broad concept. For example, Ettlinger *et al.* [5] suggest that both relatively large nanoparticles (greater than 200 nm) and very small (<5–15 nm) tend to be less harmful to the human body compared to intermediate ones (15–200 nm). The authors have explained that the larger NPs may be easily detected by the immune system and subsequently removed from the bloodstream while the smaller ones may be directly excreted through the kidneys.

With respect to MOFs, there are several studies that have found size-dependent toxicity in the nanoscale. Most of them revealed that the smaller size of NPs promoted increased toxicity due to easier penetration of physiological barriers. For example, Chen *et al.* [55] conducted cytotoxicity assessment of ZIF-8 with particle size of 50, 90 and 200 nm. Based on MTT assay they observed that when ZIF-8 concentration in HepG2 cells exceeded 14 $mg.L^{-1}$, there is a significant decrease in cell viability, the larger the smaller the MOF size. Consequently, the IC_{50} parameter reached 15.6, 17.5 and 19.7 $mg.L^{-1}$ for the 50, 90 and 200 nm ZIF-8, respectively. They also concluded that the smaller the ZIF-8 size, the higher the Zn accumulation and ROS level, resulting in a higher inflammatory response prone to inducing necrosis and/or gene up-regulation.

Particle size-dependent toxicity of MOFs was also observed by Wang *et al.* [56]. The scientists investigated the biocompatibility of 100, 200, 400, 700 and 1200 nm cobalt-based MOF (ZIF-67) to *Photobacterium Phosphoreum* T3 strain. They found that for ZIF-67 smaller than 400 nm, the toxicity increased as the particle size decreased, while no clear trend was observed for particles larger than 400 nm. This phenomenon was attributed to the fact that smaller NPs (100 and 200 nm) may enter and accumulate in the cytoplasm, thus causing severe toxicity. In turn, the role of Co^{2+} release in the toxic effect of ZIF-67 was excluded. Moreover, *in vivo* studies, performed by Deng *et al.* [57], confirmed that, contrary to 180 nm, exposure to 60 nm ZIF-67 impaired learning and memory ability in rats. It is worth highlighting that although ZIF-67 NPs were synthesized in a different way and different techniques were used to assess their biosafety, the conclusion remain the same.

Another studies presented by Hao *et al.* [58] also indicated increased cytotoxicity with regard to smaller NPs. It was reported that 30 nm Zr-based porphyrinic MOF (PCN-224) led to meaningful rupture of the cell membrane and dissolved in lysosomes, causing cell necrosis while 90 and 180 nm PCN-224 showed only a slight membrane rupture.

Particularly interesting studies was also performed by Duan *et al.* [59] who proved that the size of the drug loaded-MOF can have a completely different effect on toxicity than the free MOF. They found that 4T1 cell viability 48 h after incorporation up to 12.5 $\mu g.mL^{-1}$ amorphous ZIF-8 (AZIF-8) remains unchanged regardless of the NPs size, whereas after exposure to only 0.078 $\mu g.mL^{-1}$ of doxorubicin (DOX)-loaded AZIF-8 (DOX@AZIF-8) it drastically decreased, the more the lower the MOF size (Fig. 9a-b). Consequently, the value of IC_{50} parameter ranged from 0.068 $\mu g.mL^{-1}$ (30 nm AZIF-8) to 0.240 $\mu g.mL^{-1}$ (130 nm AZIF-8). On the other hand, for anti-cancer therapy, smaller dimensions of AZIF-8 have been shown to be more advantageous. Not only do they contribute to higher cytotoxicity, but also indicate faster release of drug (Fig. 9c-e) and greater accumulation in the tumor (Fig. 9f), resulting in more effective treatment (Fig. 9g).

Slightly different conclusions on the effect of particle size on the toxicity were provided by Wuttke *et al.* [42] who examined the 83 and 129 nm Zr-fumarate (Zr-*fum*) MOF. Although both structures did not induce considerable cytotoxicity in the LDH-assay, and no obvious morphological signs of cell death was revealed in SEM images, decreased metabolic activity was unexpectedly observed in human gingival fibroblasts and Schwann cells after exposure to larger MOF. Namely, after incubation 200 $\mu g.mL^{-1}$ of 129 nm Zr-*fum* MOF about 30% and 65% reduction in metabolic activity of gingival fibroblasts and Shwann cells was noted, respectively, while the presence of 83 nm MOF did not lead to any reduction. On the other hand, the inert behavior of the sensory neurons contained in the rat dorsal root ganglia towards 129 nm Zr-*fum* makes it a promising candidate for surface coating of nerve-guidance tubes, which cannot be said for 83 nm Zr-*fum*. Based on the presented results, it can be noticed that both MOFs show differential

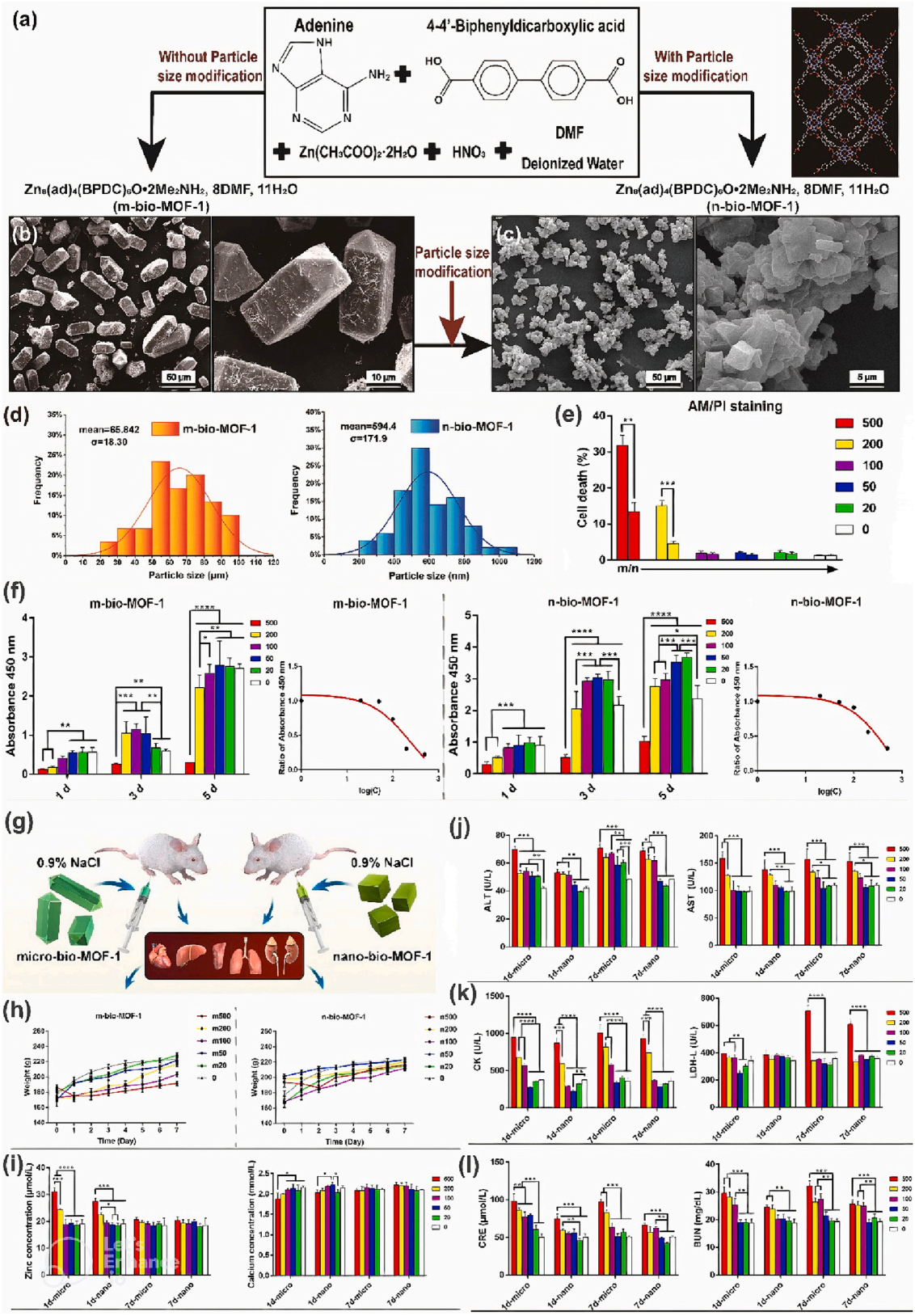

Fig. 8. *Preparation and characterization of m/n-bio-MOF-1.* (a) Synthesis. (b-c) SEM images of MOFs. (d) Particle size distribution. (e) Cytotoxicity assay. (f) CCK-8 results and corresponding curves of half inhibitory concentration. (g) Schematic depicting *in vivo* measurements. (h) Body weight. (i) Serum analysis of zinc and calcium. (j) Hepatotoxicity. (k) Cardiotoxicity. (l) Renal toxicity. Reprinted with permission from [54]. Copyright 2022 Elsevier.

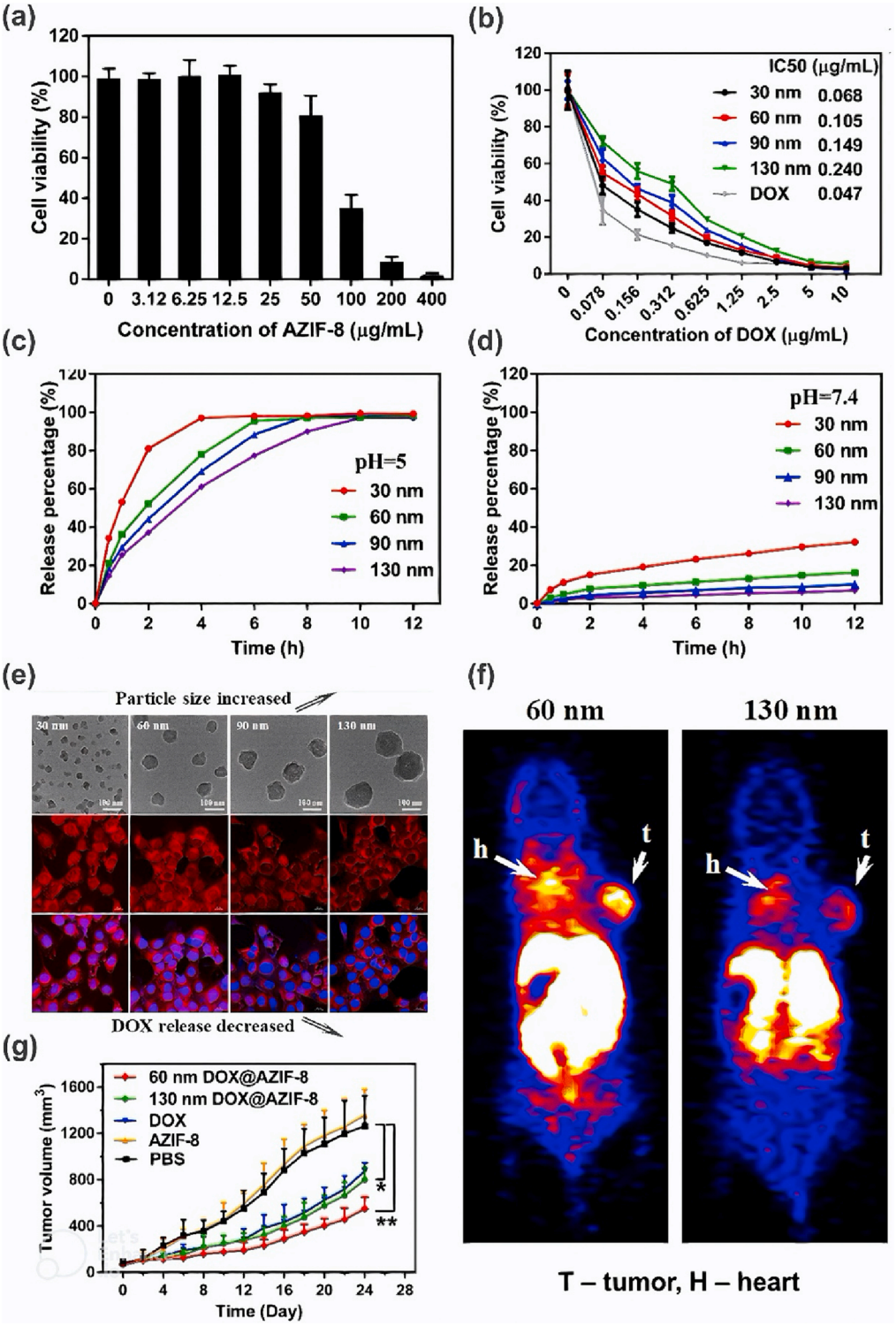

Fig. 9. *Characterization of AZIF-8 and DOX@AZIF-8.* (a) Cell viability of 4T1 cells 48 h after exposure to AZIF-8. (b) Cell viability of 4T1 cells 48 h after exposure to DOX and DOX@AZIF-8. (c-d) DOX release percentage. (e) Images of 4T1 cells incubated with DOX@AZIF-8. (f) Mice body 2 h after injection of Cu-DOX@AZIF-8 into 4T1 cells. (g) Mice tumor growth after different treatments. Reprinted with permission from [59]. Copyright 2018 American Chemical Society.

toxicity and biological response in different cells. Accordingly, despite some toxicity, they can be successfully used in specific medical applications, provided that all requirements are met.

To sum up, particle size is an important factor determining the MOF toxicity. According to the presented results, the nanometric MOFs seems to be more biocompatible compared to its micron-sized counterparts. However, considering the size of MOF NPs, it was proved that below about 200 nm, the toxicity increases with decreasing MOF size.

4.3. Morphology

Recently, several reports have shown that morphology may influence

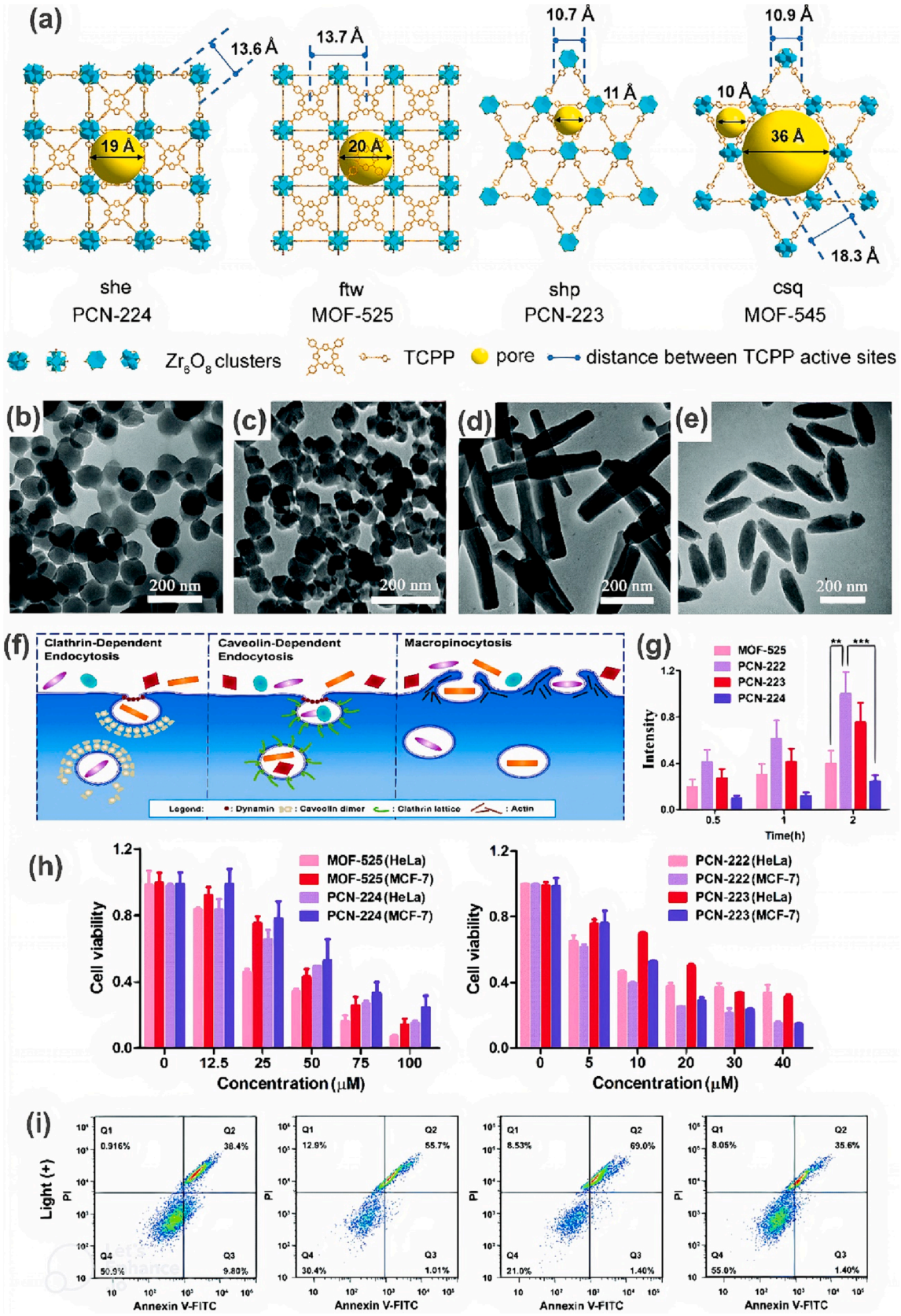

Fig. 10. *Characterization of TCPP-MOF isomers.* (a) Structures. Reprinted with permission from [60]. Copyright 2021 John Wiley and Sons. (b-e) TEM images of (b) spherical PCN-224, (c) cubic MOF-525, (d) spindle-shaped PCN-223, and (e) rod-like PCN-222 (MOF-545). (f) Endocytic pathways. (g) Cellular uptake into HeLa cells. (h) HeLa and MCF-7 cells viability after light irradiation. (i) Flow cytometry analysis, where (Q1) represents necrotic, (Q2) late-stage apoptotic, (Q3) early apoptotic, and (Q4) live cells. Reprinted with permission from [61]. Copyright 2021 Royal Society of Chemistry.

MOF toxicity. Although two independent studies on the shape effect of the porphyrinic zirconium MOFs (TCPP-MOFs): spherical PCN-224, cubic MOF-525, spindle-shaped PCN-223, and rod-like PCN-222 (other name MOF-545) (Fig. 10b-e) have been conducted, no agreement was observed between the published results. As both research groups analyzed MOFs with photodynamic therapy in mind, the reported toxicity results are for cells exposed to light irradiation (no notable toxicity was observed without irradiation).

For example, Liu *et al.* [60] found that bacterial viability of *E. coli* and *S. aureus* decreased under irradiation with the increasing concentration of MOF, with the highest reduction observed for rod-like, cubic, spherical, and finally spindle-shaped TCPP-MOF, respectively. *E. coli* and *S. aureus* viability after incubation with 100 $\mu g.mL^{-1}$ MOF was 0.3, 13.7, 32.3, 35.3 % and 0.2, 0.6, 5.0, 9.3%, according to the above order. These results were consistent with $^1O_2$ production level in individual MOF incubated bacteria. Authors claims that the better performance for ROS generation (and thus higher toxicity) is associated with larger pore size and longer distance of TCPP activity sites, which was visualized in Fig. 10a.

On the other hand, Zhou *et al.* [61] observed slightly different dependency between the TCPP-MOF topology and cytotoxicity against HeLa and MCF-7 cells. In particular, they showed considerably lower cell viability after exposure to rod- or spindle-shaped MOFs in contrast to cubic or spherical structures at the same concentration and irradiation, as shown in Fig. 10*h*. Photodynamic IC_{50} value was calculated to be 7.4–10.9, 12.5–18.8, 27.8–43.4, and 40.4–52.8 μM for PCN-222, PCN-223, MOF-525, and PCN-224, respectively, depending on the cell tested. Higher amount of necrotic and/or apoptotic cells induced by irregularly shaped TCPP-MOF was reported based on flow cytometry analysis as well (Fig. 10i). According to the authors, this phenomenon results from the fact that MOFs can undergo selective endocytic pathways depending on the topology (Fig. 10f), and consequently determine the internalization efficiency. Accordingly, longitudinal TCPP-MOFs, undergoing macropinocytosis as a major endocytic route, penetrate HeLa cells much more easily than regular-shaped ones (Fig. 10g), which translates into higher cytotoxicity. Interestingly, no significant histopathological abnormalities or inflammatory responses to any type of TCPP-MOF were detected during the mice examination.

Hao *et al.* [58] also examined the shape effect of rod-like and spherical TCPP-MOFs on macrophage toxicity, but surprisingly, came to yet other conclusions. Contrary to previous works [60,61] which found the rod-like TCPP-MOF to be the most toxic, they demonstrated that spherical MOF gave stronger inhibition of cell viability and led to more significant cell necrosis induced by lysosome damage than rod-shaped MOF. The effect of topology was also studied by Tamames-Tabar *et al.* [45], however its influence was not significant.

In light of the presented findings, it can be concluded that morphology may significantly affect MOF toxicity due to, for instance, other endocytic pathways or different pore sizes. However, it is still difficult to indicate a specific trend.

4.4. Zeta potential/particle aggregations

Zeta potential (ζ-potential) is a parameter related to the charge present on the surface of particles. Its value determines the electrostatic repulsion force responsible for colloids stabilization. It is known that a strongly negative or positive zeta potential provides appropriate colloidal stability, while a more neutral one (absolute potential value below 30 mV) leads to easy aggregations due to physical instability of the system [62]. As observed in the past, weak zeta potential results in increased toxicity of various NPs [63]. Therefore, we assume that this may influence MOF toxicity as well. Although, few studies have paid attention to the role of zeta potential and/or aggregation on the MOF toxicity, we will try to discuss this as thoroughly as possible.

Interesting research was carried out by Zimpel *et al.* [64], who functionalized Zr-*fum* using different polymer coatings and investigated the effect of variable zeta potential on protein binding and cellular interactions (see schematic illustration in Fig. 11a-b). The results of dynamic light scattering performed in HEPES buffered glucose (HBG) solution (simulation of the physiological cell culture pH) revealed that cationic polymer coated Zr-*fum* was more aggregated compared to the Zr-*fum* coated with anionic polymer or without any coating. This phenomenon was corresponded to the measured zeta potential values, which were minus 11–16 and minus 25–30, respectively. However, it should be noted that colloid stability is highly dependent on pH as can be seen in Fig. 11c. Consequently, MOF NPs can be tolerated differently by different physiological centers of the human body. Nevertheless, in this study, all measurements were conducted in the previously mentioned HBG solution. Based on data presented in Fig. 11d, it can be seen that no obvious toxicity was induced in HeLa cells under the influence of up to 400 $\mu g.mL^{-1}$ of various Zr-*fum*. However, deeper explorations revealed other abnormalities. It was found that more negatively charged Zr-*fum* were internalized into cells, while cationic-coated Zr-*fum* showed strong aggregation on the cell surface (membrane binding) and thus low intracellular localization (Fig. 11e-f). As we explained in the section 3, cell surface adsorption of NPs is one of the toxicity mechanisms as it is likely to cause membrane damage, confirming the negative impact of weak colloidal stability on the safety of MOF-incubated biological systems.

On the other hand, Grall *et al.* [40] demonstrated that although Cr-based MIL-100 showed higher aggregation and a more neutral zeta potential in cell culture media (DMEM and MEM) compared to MIL-100 (Fe) and MIL-100(Al), all MOFs induced no significant toxicity after the contact with biological media. However, in our opinion, the difference between zeta potential of considered MOFs was not critical, since it ranged from −12 to −4 mV, so the influence of the aggregations and surface charge on the toxicity of MIL-100 cannot be excluded. Additionally, there are several other studies that have measured zeta potential but found no correlation between toxicity [41,45].

In conclusion, there are some indications that aggregations may influence MOF toxicity and the zeta potential may be the first tool to assess/detect this toxicity. However, based on the available studies, due to the large number of variables, it is difficult to estimate the real contribution of this parameter to the safety of biological systems. So far, surface charge has usually been ignored in favor of other determining factors. Nevertheless, we believe that zeta potential is responsible for many characteristics of MOF, and its change through the appropriate functionalization could provide an opportunity to design MOF with controlled tissue binding and colloid stability of individual physiological media. Accordingly, more specific MOF toxicity examinations targeting the role of this parameter are highly recommended.

4.5. Summary

To summarize all data on the assessment of the toxic behavior of individual MOFs, considering various factors, we prepared a comprehensive table (Table 1). Overall level of toxicity and its change under the influence of specific parameter, as well as the type of studied model/cells and performed measurements can be read from the Table. According to the current state of knowledge, less toxic MOFs seems to be MIL-100, MIL-127, UiO-66, UiO-67, MIL-101, MIL-88B, MOF-74 composed of one of the following metal nodes: Mg, Zr, Cr, Co, Al, Fe. Nevertheless, biosafety evaluation of other not well-studied MOFs is also highly desirable. In addition, special attention should be paid to the size of MOF during designing, since smaller NPs (with diameter sizes < 200 nm) seem to be more severe to living organisms. However, the influence of morphology and zeta potential needs further investigation.

5. Strategies to reduce MOF toxicity

In a previous section, the role of physico-chemical properties of MOFs on their toxicity was discussed. It was found that features such as

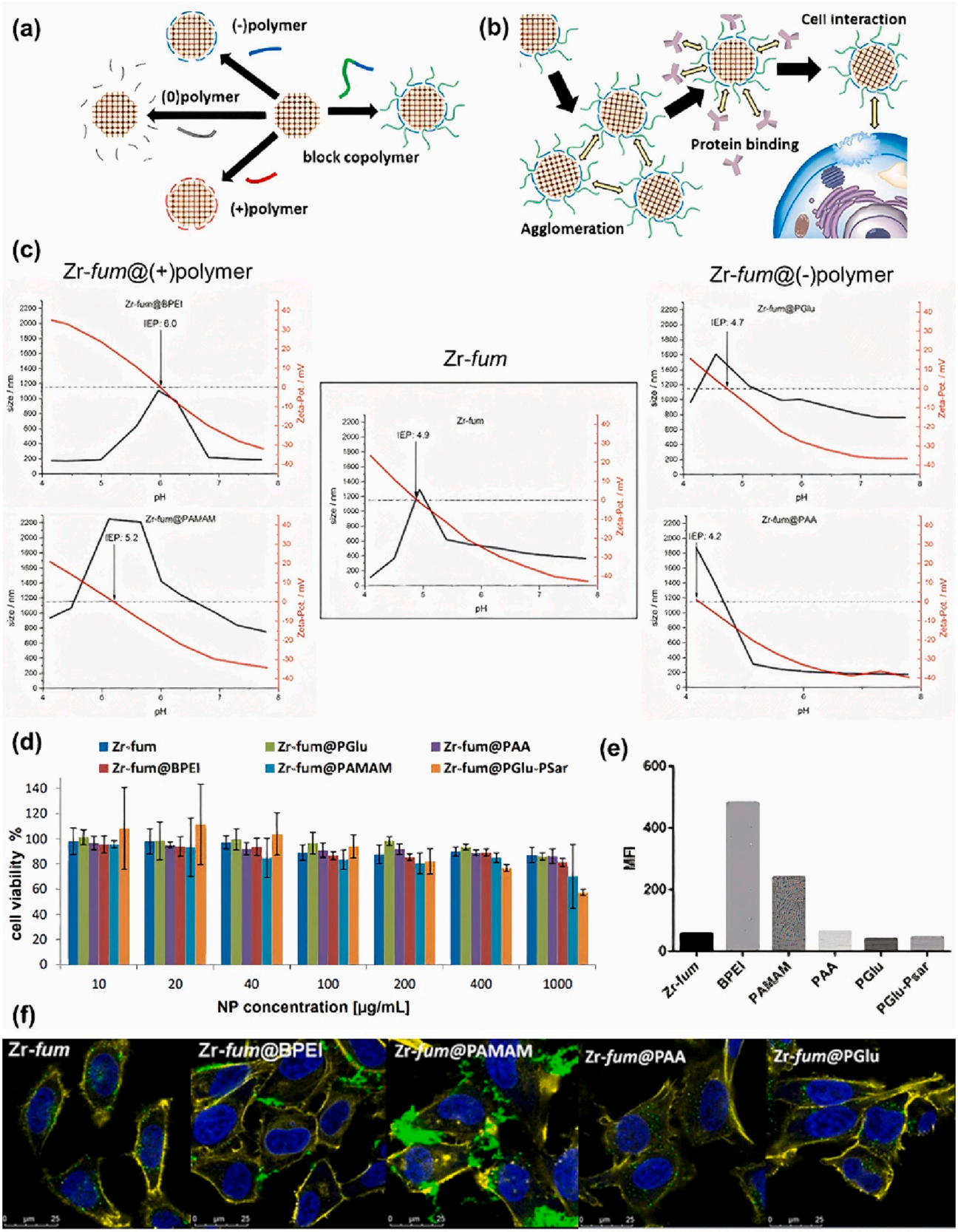

Fig. 11. *Characterization of Zr-fum.* (a) Schematic illustration of Zr-*fum* functionalization, and (b) its performance. (c) Average size and zeta potential of Zr-*fum* and functionalized Zr-*fum* as a function of pH. (d) HeLa cell viability 24 h following MOF treatment. (e) Median fluorescence intensities of calcein-positive cell sub-population. (f) Confocal images depicting HeLa cells. Blue, yellow, and green colors correspond to nuclei stained with DAPI, F-actin stained with phalloidin-rhodamine, and calcein, respectively. Reprinted with permission from [64]. Copyright 2019 American Chemical Society. (For interpretation of the references to color in this figure legend, the reader is referred to the web version of this article.)

Table 1
Effect of physico-chemical factors on MOF toxicity.

MOF	Study model	Cells/animal	Toxicological assay	Factor determining the toxicity	Comment/Main outcome	Refs.
MOF-74	*In vitro*	HepG2 MCF7	Cell viability	Metal (Zn, Cu, Ni, Co, Mn, Mg)	MOF-74 containing Cu and Mn showed high toxicity, Zn-MOF-74 showed medium toxicity, while MOF-74 composed of Co, Ni, and Mg showed minor toxicity	[37]
MOF-74	*In vivo*	Zebrafish embryos	Morphological defects	Metal (Co, Mg)	Co-MOF-74 resulted in yolk sac edema of embryos; however, Mg-MOF-74 did not induce any toxicity	[37]
MOF-5 UiO-66	*In vitro*	HepG2 MCF7	Cell viability	Metal (Zn, Zr)	Minor toxicity of UiO-66(Zr), and moderate toxicity of MOF-5(Zn)	[37]
MIL-100 HKUST-1	*In vitro*	HepG2 MCF7	Cell viability	Metal (Fe, Cu)	Moderate toxicity of MIL-100(Fe), and high toxicity of HKUST-1(Cu)	[37]
MIL-100 HKUST-1	*In vivo*	Zebrafish embryos	Hatching rate Morphological defects	Metal (Fe, Cu)	Moderate toxicity of MIL-100(Fe), and high toxicity of HKUST-1(Cu)	[37]
ZIF-8 ZIF-67	*In vitro*	Red blood cell	Hemolysis assay	Metal (Zn, Co)	Co-based ZIF-67 caused significant hemotoxicity while Zn-based ZIF-8 was hematocompatible	[38]
MIL-100	*In vitro*	A549 Calu-3 HepG2 Hep3B	Cell viability ROS level Cell cycle analysis Genotoxicity	Metal (Fe, Al, Cr)	No toxic effect of Al-, and Cr-based MOF. Only slight toxicity against Hep3B cell after exposure to 100 μg.mL^{-1} MIL-100(Fe)	[40]
MIL-100	*In vitro*	J774.A1 peripheral blood mononuclear cells	Cell viability ROS production Cytokine production	Metal (Fe, Al)	No evident toxicity of both MOFs, however an increase in production of pro-inflammatory cytokines was observed	[41]
MIL-100, MIL-101	*In vitro*	HMEC HUVEC MLE12 MH-S Gingival Fibroblasts Human Schwann cells	Apoptosis rate Inflammatory response Metabolic activity Cell viability	Metal (Fe, Cr)	Minor toxicity of MIL-101(Cr) and moderate toxicity of MIL-100(Fe). Toxicity significantly increases after exposure to 100 μg.mL^{-1} MIL-100(Fe) and 200 μg.mL^{-1} MIL-100(Cr)	[42]
PCN-333	*In vitro*	HDF 3 T3 HeLa *S. aureus* *E. coli* *P. aeruginosa*	IC_{50} Hemolysis assay Minimum inhibitory concentration	Metal (Fe, Al)	Comparably minor toxicity of both MOFs	[43]
MIL-101 MIL-53 UiO-66	*In vitro*	HDF 3 T3 HeLa *S. aureus* *E. coli* *P. aeruginosa*	IC_{50} Hemolysis assay Minimum inhibitory concentration	Metal (Fe, Al, Zr)	Comparably minor toxicity of these MOFs	[43]
CIM-80 CIM-84	*In vitro*	J774.A1	IC_{50}	Metal (Al, Zr)	Both MOFs did not show any toxicity up to 5000 μg.mL^{-1}	[44]
CIM-80 CIM-84	*In vivo*	Amphipods	Survival assay	Metal (Al, Zr)	In both cases all animals survived after exposure to 5000 μg.mL^{-1} MOFs	[44]
MIL-88B UiO-66 ZIF-8	*In vitro*	J774 HeLa	IC_{50}	Metal (Fe, Zr, Zn)	Toxicity increased in the following order: Fe < Zr < Zn	[45]
MIL-127 MIL-100 MIL-101 MIL-88A MIL-88B	*In vitro*	HeLa J774	IC_{50}	Organic linker (TAZB, BTC, FUM, BDC, BDC-CH_3, BDC-$2CH_3$, BDC-$4CH_3$, BDC-$2CF_3$, BDC-NH_2, BDC-NO_2	Toxicity highly dependent on the tested cell line. All MOFs, except for MIL-88A composed of fumaric acid were biocompatible with HeLa cell. The IC50 value towards J774 cells ranged from 30 to 700 μg.mL^{-1}, while the highest toxicity was observed for MOFs containing BDC-NO_2, FUM, BDC-NH_2, BDC-$4CH_3$, BDC-$2CH_3$.	[45]
MIL-100 MIL-88A MIL-88B-$4CH_3$	*In vivo*	Rats	Survival assay Histological examination	Organic linker (BTC, FUM, BDC-$4CH_3$)	Low toxicity of all MOFs	[46]

(*continued on next page*)

Table 1 (*continued*)

MOF	Study model	Cells/animal	Toxicological assay	Factor determining the toxicity	Comment/Main outcome	Refs.
UiO-64 UiO-66	*In vitro*	J774.A1	IC_{50}	Organic linker (FUM, BDC)	Both MOFs did not show any toxicity up to 5000 $\mu g.mL^{-1}$	[44]
UiO-64 UiO-66	*In vivo*	Amphipods	Survival assay Mobility	Organic linker (FUM, BDC)	All animals incubated with 2500 $\mu g.mL^{-1}$ UiO-66 (BDC) survived but showed reduced mobility while most amphipods died after exposure to UiO-64 (FUM)	[44]
MIL-100 MIL-101-NH_2	*In vitro*	HepG2 MCF7	Cell viability	Organic linker (BTC, BDC-NH_2)	Moderate toxicity of both MOFs, however slightly higher for MIL-100 (BTC)	[37]
MIL-100 MIL-101-NH_2	*In vivo*	Zebrafish embryos	Hatching rate Morphological defects	Organic linker (BTC, BDC-NH_2)	Moderate toxicity of MIL-100 (BTC), and high toxicity of MIL-101-NH_2 (BDC-NH_2)	[37]
UiO-66 UiO-66_NH_2	*In vitro*	HepG2 MCF7	Cell viability	Organic linker (BDC, BDC-NH_2)	UiO-66-NH_2 induced higher toxicity towards HepG2 cell, and lower towards MCF7 cell compared to UiO-66	[37]
ZIF-8 ZIF-7	*In vitro*	HepG2 MCF7	Cell viability	Organic linker (MI, IM)	Moderate toxicity of ZIF-7 (IM), and high toxicity of ZIF-8 (MI)	[37]
ZIF-8 ZIF-7	*In vivo*	Zebrafish embryos	Hatching rate Morphological defects	Organic linker (MI, IM)	Moderate toxicity of ZIF-7 (IM), and high toxicity of ZIF-8 (MI)	[37]
ZIF-90	*In vitro*	HEK-293 MCF-7	Cell viability IC_{50}	Organic linker (differing by aldehyde, carboxyl, amino, thiol group)	Minor toxicity of all MOFs. The toxicity increased in the following order: amino-, thiol-, carboxyl-modified MOF, unmodified MOF	[47]
PCN-333(Fe) MIL-101 (Fe) MIL-100 (Fe)	*In vitro*	HDF 3 T3 HeLa RBC	IC_{50} Hemolysis assay	Organic linker (TATB, BDC, BTC)	Low toxicity of all MOFs	[43]
PCN-333(Fe) MIL-101 (Fe) MIL-100 (Fe)	*In vivo*	Mice	Skin penetration assay	Organic linker (TATB, BDC, BTC)	No toxicity of all MOFs	[43]
PCN-333(Al) MIL-53(Al)	*In vitro*	HDF 3 T3 HeLa	IC_{50} Hemolysis assay	Organic linker (TATB, BDC)	Low toxicity of all MOFs	[43]
PCN-333(Al) MIL-53(Al)	*In vivo*	Mice	Skin penetration assay	Organic linker (TATB, BDC)	No toxicity of all MOFs	[43]
MOF-808 (Zr) UiO-66(Zr)	*In vitro*	HDF 3 T3 HeLa	IC_{50} Hemolysis assay	Organic linker (BTC, BDC)	Low toxicity of all MOFs	[43]
MOF-808 (Zr) UiO-66(Zr)	*In vivo*	Mice	Skin penetration assay	Organic linker (BTC, BDC)	No toxicity of all MOFs	[43]
Mg-MOF74	*In vitro*	HeLa	Cell viability, IC_{50} Apoptosis assay Cell phagocytosis	Size (nano/micro)	n-Mg-MOF74 causes toxicity above 1000 $\mu g.mL^{-1}$ and m-Mg-MOF74 above 500 $\mu g.mL^{-1}$	[53]
Mg-MOF74	*In vivo*	Rats	Body weight examination Blood biochemistry assay Histological examination	Size (nano/micro)	no significant evidence of toxicity, n-Mg-MOF74 shows lower cardiotoxicity and less effect on the body growth compared to m-Mg-MOF74	[53]
Bio-MOF-1	*In vitro*	MC3T3-E1	Cell proliferation IC_{50} Cell death rate Apoptosis assay	Size (nano/micro)	Both nano and micro bio-MOF-1 causes toxicity above 100 $\mu g.mL^{-1}$, however among them n-bio-MOF-1 shows better biocompatibility	[54]

(*continued on next page*)

Table 1 (*continued*)

MOF	Study model	Cells/animal	Toxicological assay	Factor determining the toxicity	Comment/Main outcome	Refs.
Bio-MOF-1	*In vivo*	Rats	Weight examination Blood biochemistry assay Histological observation	Size (nano/micro)	Both nano and micro bio-MOF-1 causes toxicity from 100 $\mu g.mL^{-1}$, however among them n-bio-MOF-1 shows better biocompatibility	[54]
ZIF-8	*In vitro*	HepG2	Cell viability IC_{50} ROS generation Inflammation Death mode	Size (50, 90 and 200 nm)	Certain toxicity of ZIF-8. The lower the MOF size, the higher the toxicity	[55]
ZIF-67	*In vitro*	*Photobacterium phosphoreum* T3 strain	Luminescence inhibition rate	Size (100, 200, 400, 700 and 1200 nm)	Strong toxicity after incubation of 5 $mg.L^{-1}$ ZIF-67. For ZIF-67 smaller than 400 nm, the toxicity increased as the particle size decreased, while no clear trend was observed for particles larger than 400 nm	[56]
ZIF-67	*In vivo*	Rats	Weight examination Morris water maze test Histopathological examination Transcriptomic exploration	Size (60, 180 nm)	Only 60 nm ZIF-67 caused the impairment of learning and memory ability	[57]
Zr-*fum* MOF	*In vitro*	Human gingival fibroblasts Human Schwann cells Rat dorsal root ganglion cultures	Metabolic activityToxicity (LDH-assay) Sensory neurons response	Size (83, 129 nm)	Only minor signs of cytotoxicity. Larger MOF has lower metabolic activity but smaller reduced the neurite outgrowth	[42]
TCPP-MOF	*In vitro*	*E. coli* *S. aureus*	Bacterial viability $^1O_2$ production	Shape (cubic, rod-like, spindle, spherical)	Certain toxicity of TCPP after light irradiation. Shape-dependent toxicity was found. Toxicity decreases in the following order: rod-like > cubic > spherical > spindle-shaped TCPP-MOF	[60]
TCPP-MOF	*In vitro*	HeLa MCF-7	Cell viability Flow cytometry analysis	Shape (cubic, rod-like, spindle-shaped, spherical)	Certain toxicity of TCPP after light irradiation. Higher toxicity of rod- and spindle-shaped TCPP-MOFs compared to cubic and spherical	[61]
TCPP-MOF	*In vivo*	Mice	Body weight examination Blood biochemistry assay Histological examination	Shape (cubic, rod-like, spindle, spherical)	No significant toxicity to any type of TCPP-MOF	[61]
Zr-*fum*	*In vitro*	HeLa	Cell viability Cellular association	Zeta potential (-11 ÷ -16, -25 ÷ -30)	Lower internalization and higher cell surface adsorption observed for MOF with lower zeta potential	[64]
MIL-100	*In vitro*	A549 Calu-3 HepG2 Hep3B	Cell viability ROS generation Cell cycle analysis DNA damage	Zeta potential (~-5 mV, ~ -10 mV)	All MOFs induced no significant toxicity	[40]

chemistry, particle size, morphology, and aggregation significantly determine MOF biocompatibility. Therefore, the appropriate design and some manipulation of aforementioned parameters can effectively mitigate the inherent harmfulness of these structures, providing a better potential in biomedical applications. However, it is important to note that even a meticulously planned model with a specific set of properties cannot ensure its complete safety for living organisms. Accordingly, in this section, we propose various strategies to reduce MOF toxicity, regardless of their physico-chemical properties. These strategies include green chemistry and/or surface modifications.

5.1. Green chemistry

Altering MOF chemistry through the selection of green ligands, linkers, and solvents is a potential strategy to mitigate toxicity. However, this approach can be challenging, as the use of natural/green equivalents usually involves a deterioration in performance and functionality of MOFs. Nevertheless, in recent years, many efforts have been made to design, synthesize, and study the effectiveness of green MOFs for biomedical applications. Our group has previously reviewed these studies [65].

Although a lot of data is available, very little is relevant to the toxicity assessment of green MOFs. One of the meaningful studies was provided by Grape *et al.* [66] who suggest that the use of green components, in particular solvents and ligands, allows for obtaining completely biocompatible and environmentally-friendly MOFs. To prove this, the scientists designed and synthesized green MOF, SU-101, composed of renewable phenol-functionalized and plant-based linkers and bismuth ions. For this purpose, ellagic acid isolated from chestnut tree bark and pomegranate hulls was utilized. The synthesis was carried out in water at ambient temperature. As expected, very low cytotoxicity of this structure was observed against HL-60 cells even after exposure to 1000 $\mu g.mL^{-1}$ SU-101. In addition, the synthesized MOF exhibited adequate colloidal stability in water, corresponding to a strongly negative zeta potential (-35 mV). The authors suggested that the stability may be due to the presence of partially coordinated ellagate anions or hydroxyl groups on the MOF surface.

Similar approach was presented by Abuçafy *et al.* [67]. It was confirmed that MOF containing cyclodextrin (CD) (semi-natural product obtained from starch) as an organic linker induced no toxicity in HepG2 and Caco-2 cells up to 2000 $\mu g.mL^{-1}$ (average cell viability greater than 100%), regardless of the metal node (K, Na, Fe). It is worth mentioning that this is the highest concentration possible to estimate, as it corresponds to the dispersion limit of MOF in DMEM. Importantly, the obtained results demonstrated a good ability of the CD-based MOF to incorporate a high amount of drug (the entrapment efficiency of 49–55%) and its controlled release. In addition, *in vivo* anti-inflammatory activity of the drug-loaded MOFs was examined. It was revealed that all MOF-treated mice exhibited the same inhibition of inflammation as the drug positive control, expect for mouse incubated with Fe-based MOF. The effectiveness of the paw edema inhibition after 24 h was <90% for Fe-based MOF, and 17–30% for the other samples, which gives hopes for drug delivery applications.

To the best of our knowledge, there is only one study comparing the biomedical utility of conventionally synthesized MOF against its counterpart built from environmentally friendly components. Agostoni *et al.* [68] performed a hydrofluoric acid (HF)-free synthesis route of MIL-100 (Fe) using iron(III) chloride hexahydrate instead of Fe^0 metal and compared the physico-chemical properties of MOF obtained by the green and conventional methods. The results indicated that the crystallinity, particle size and surface area of MIL-100 remain the same after using both techniques. However, the HF-free MOF had even better drug encapsulation efficiency (~99) and was able to release it in a progressive manner. Moreover, no significant cytotoxicity was observed after administration of the HF-free MOF to J774.A1 cells (IC_{50} = 300 $\mu g.mL^{-1}$). Although, the toxicity of conventionally synthesized MOF was not examined, it can be concluded that green MIL-100(Fe) is at least as biocompatible as its conventional version. However, it is also worth mentioning that this green procedure not only eliminated the use of toxic HF, but also brought other benefits such as increased the yield (80% instead of 8%) and shortened the synthesis time (6 min instead of 30 min).

On the other hand, we found an indication in the literature that bio-derived MOF do not necessarily have to be biosafe. This opinion was provided by Jiang *et al.* [54] who synthesized bio-MOF-1 using bio-derived components fabricated by zinc-adeninate SBUs and green DMF solution. The toxicological experiments revealed that despite biosafe composition, bio-MOF-1 exhibited certain *in vitro* and *in vivo* toxicity at higher concentrations (greater than 100 $\mu g.mL^{-1}$). More detailed results of this work have already been discussed in section 4.2 and presented in Fig. 8. Based on the provided information, it can be concluded that green approach in the synthesis of MOF is not synonymous with full biocompatibility of this structure, especially since the toxicity is a very complex feature. Nevertheless, it is widely known that green components contribute to increased biological safety of materials, and their use is highly appreciated, even from an environmental point of view. Besides, they are likely to help reduce the toxicity, at least to some extent. However, further research is needed to confirm the superiority of green MOFs over conventional structures in terms of non-toxicity and utility in biomedical applications.

5.2. Surface modification

In addition to green precursors and/or solvents, surface modifications also play an important role in reducing the toxicity of MOFs. Surface properties govern the interactions between framework and biological environment, therefore their appropriate modification may limit the direct contact of MOF with the surface of cells [69]. So far, several types of modifications have been shown to be beneficial from a MOF biosafety point of view. The most promising ones include coating with biomolecules and surface modification through covalent bonding.

Several researchers have confirmed the effectiveness of improving the biosafety of MOFs by modifying them with lipids. For example, Wuttke *et al.* [42] showed that the presence of a lipid bilayer (1,2-dioleoyl-*sn-glycero*-3-phosphocholine, DOPC) around MIL-100(Fe) and MIL-101(Cr) NPs increases their biocompatibility. Nevertheless, at high doses (100 $\mu g.mL^{-1}$), it still exhibits some toxicity to epithelial cells. On the other hand, Ploetz *et al.* [70] revealed reduced viability of HeLa cells after exposure to lipid-coated MIL-100, however, it was considered that the lower toxicity of uncoated MIL-100 results from lower cellular internalization. It is worth mentioning that coating MIL-100(Fe) and MIL-101(Cr) with DOPC increases the uptake efficiency of MOF by cancer cells and prevents their premature release, making these nanocarriers promising for drug delivery applications [71]. The most beneficial effect of lipid-functionalization of PCN-223 was observed by Yang *et al.* [72]. In the schematic illustration in Fig. 12a, the authors listed cellular stability, biocompatibility, and uptake rate as the most important features that were improved. Selected results, referring to the above-mentioned analyses are shown in Fig. 12b-i. TEM images (Fig. 12c-d) revealed that contrary to the coated MOF, bare PCN-223 crystals underwent serious corrosion after keeping in PBS (simulative physiological solution) for 2 days. This was consistent with the XRD measurement, which confirmed the amorphous character of unmodified NPs (Fig. 12b). On the other hand, as can be seen in Fig. 12e, the lipid-coated PCN-223 remains stable in PBS solution for at least 7 days. Furthermore, MOF with lipid bilayer induced lower cytotoxicity against SMMC-7721 and HeLa cells (Fig. 12f-g), despite higher cellular internalization (Fig. 12h-i).

MOFs coated with other biomaterials such as heparin, or chitosan have also been studied. For example, Hidalgo *et al.* [73] found that chitosan-modified MIL-100 had better chemical stability and showed reduced production of pro-inflammatory cytokines from peripheral

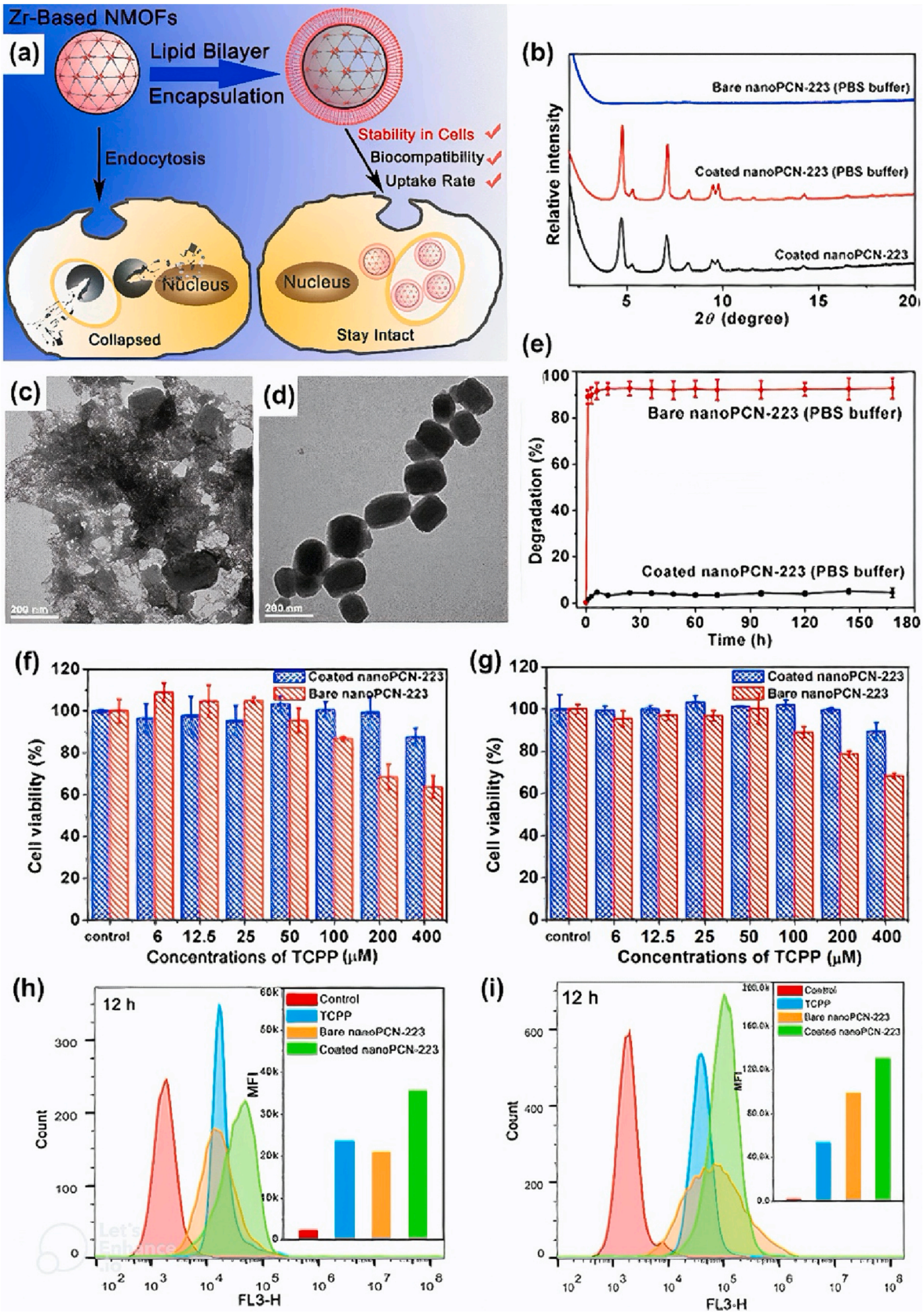

Fig. 12. *Characterization of PCN-223.* (a) Schematic illustration of PCN-223 with and without lipid bilayer. (b) XRD analysis of PCN-223. (c-d) TEM images of PCN-223: (c) and lipid-coated PCN-223 and (d) after 2-day incubation in PBS solution. (e) Degradation rate of PCN-223. Hepatocarcinoma SMMC-7721 (f) and HeLa (g) cell viability 24 h after PCN-223 incubation. Flow cytometry of hepatocarcinoma SMMC-7721 (h) and HeLa (i) cells 12 h after PCN-223 incubation. Reprinted with permission from [72]. Copyright 2017 American Chemical Society.

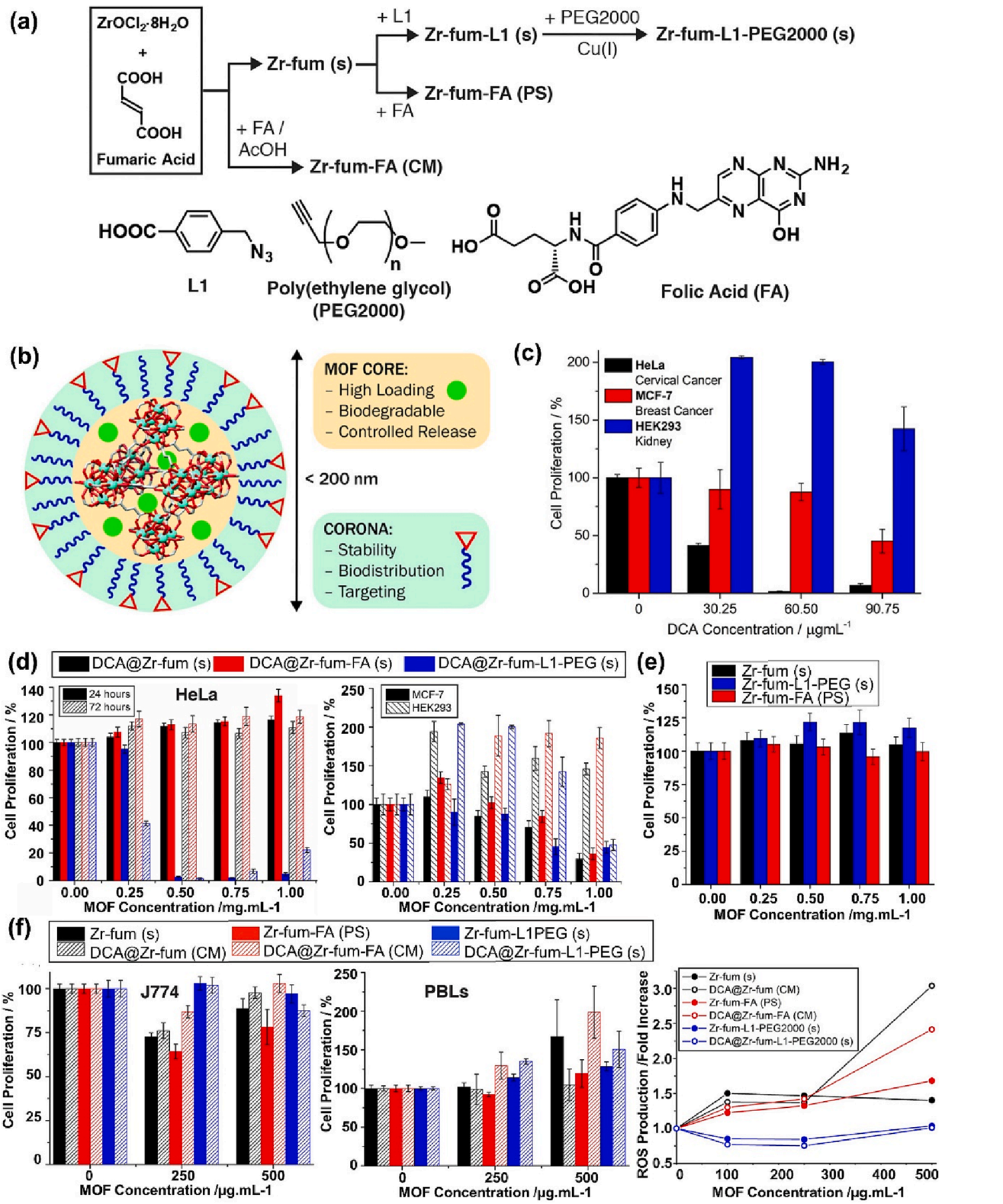

Fig. 13. *Characterization of Zr-fum pre- and post-surface modification.* (a) Synthesis scheme of modified Zr-*fum*. (b) Schematic illustration of the Zr-*fum* structure, divided into two main parts, each of which is responsible for different properties. (c) Selective anticancer cytotoxicity of PEGylated Zr-*fum* in the presence of drug. (d) Toxicity of DCA-loaded Zr-*fum* with or without modification. (e) Toxicity of Zr-*fum* toward HeLa cells 72 h after incubation. (f) Toxicity induced 72 h after exposure to loaded and unloaded-Zr-*fum*. (g) ROS generation. Reprinted with permission from [82]. Copyright 2018 American Chemical Society.

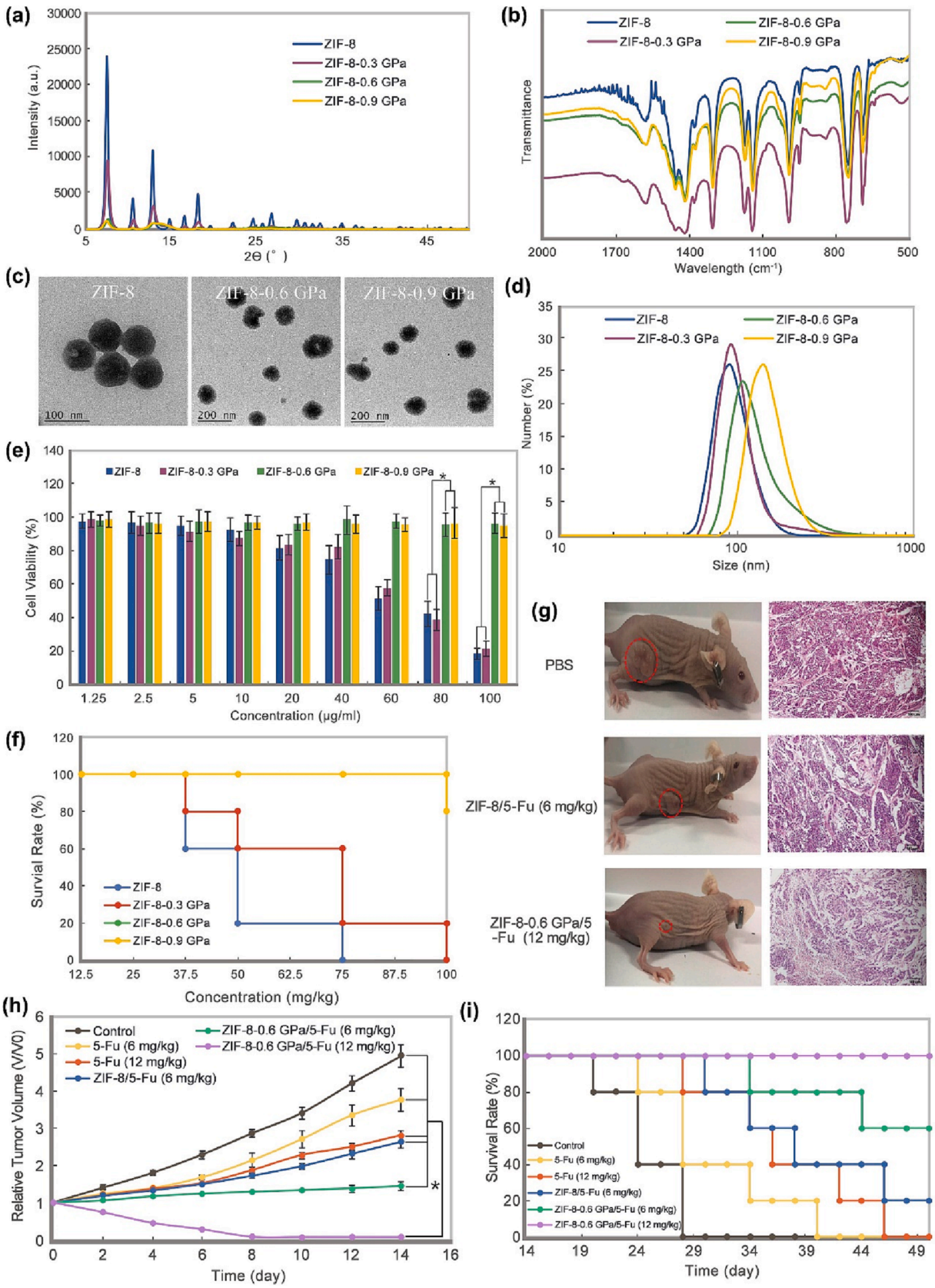

Fig. 14. *Characterization of ZIF-8 pre- and post-amorphization.* (a) XRD analysis, (b) FT-IR analysis (c) TEM images, (d) DLS analysis of ZIF-8 (pre-amorphization) and ZIF-8–0.3GPa, ZIF-8–0.6GPa, and ZIF-8–0.9GPa (post-amorphization). (e) ECA-109 cell viability 24 h after ZIF-8 incubation (pre- and post-amorphization), (f) Mouse survival rate at day 1 following ZIF-8 (pre- and post-amorphization) inoculation at various concentrations (12.5–100 mg/Kg), (g) Photos of tumor-bearing mice at day 14 following treatment with PBS (placebo), ZIF-8 filled with fluorouracil (5-Fu) anticancer drug, and amorphous ZIF-8 filled with 5-Fu, (h) Relative tumor volume over time, and (i) Mice survival rate over time. Reprinted with permission from [104]. https://creativecommons.org/licenses/by/4.0/.

Table 2
Toxicity of non-modified and modified MOFs.

MOF	Study model	Cells/animal	Toxicological assay	Way of reducing the toxicity	Comment/Main outcome	Refs.
MIL-100 (Fe) MIL-101 (Cr)	*In vitro*	HMEC HUVEC MLE-12 MH-S	Apoptosis rate Inflammatory response Metabolic activity Cell viability	Lipid coating	Lipid coating slightly reduced the toxicity of MOFs.	[42]
MIL-100 (Fe)	*In vitro*	HeLa	Cell viability Cell uptake	Lipid coating	Lipid-coated MOF induced higher toxicity compared to the bare MOF, but also increased cellular uptake.	[70]
PCN-223	*In vitro*	SMMC-7721 HeLa	Cell viability Degradation rate Flow cytometric analysis	Lipid coating	Lipid coating improved biocompatibility, cellular stability, and uptake rate of MOF.	[72]
MIL-100 (Fe)	*In vitro*	Caco-2Peripheral blood mononuclear cells (PBMCs)	Cell viability Colloidal stability Cytokine production	Chitosan coating	Chitosan coating improved chemical stability and reduced immunological response. Both coated and uncoated MOF induced almost no toxicity.	[73]
MIL-100 (Fe)	*In vitro*	J774.A1	Cell viability Colloidal stability ROS generation Cytokine production	Heparin coating	Both coated and uncoated MOF induced almost no toxicity.	[74]
UiO-66-NH_2	*In vitro*	HEK-293 HeLa HepG2 PC12 MCF-7 HT-29	Cell viability	Surface modification with benzamide-like molecules based on *Citrus tangerine* leaf extract	MOF modified with leaf extract induced lower toxicity.	[75]
Zr-*fum*	*In vitro*	HeLa MCF-7 HEK293 J774 PBLs	Cell viability ROS generation	Surface modification with PEG or FA	Drug-loaded MOF modified with PEG exhibited selective toxicity: high toxicity to cancer cells and low toxicity for non-cancer cells. Negligible effect of FA modification.	[82]
HKUST-1	*In vitro*	HEKas HDFs	Cell viability	Surface modification with FA	FA modification reduced the toxicity of MOF.	[83]
HKUST-1	*In vivo*	Diabetic mice	Wound healing Body weight examination Histopathological assay	Surface modification with FA	FA modification reduced the toxicity of MOF.	[83]
HKUST-1	*In vivo*	Mice	Blood biochemistry assay Hormone assessment Reproductive system examination Histological examination Gene expression analysis	Surface modification with FA	FA modification reduced the toxicity of MOF.	[84]
ZIF-8	*In vitro*	HepG2	Cell viability ROS generation	Surface modification with HA	HA modification reduced the toxicity of MOF.	[102]
ZIF-8	*In vivo*	Mice	Hematological examination Histological examination	Surface modification with HA	HA modification reduced the toxicity of MOF.	[102]
MOF-199	*In vitro*	White-rot fungus *Phanerochaete chrysosporium*	Weight growth examination Enzyme activity ROS generation	Carbonization	Carbonization reduced the toxicity of MOF.	[103]
ZIF-8	*In vitro*	ECA-109 MCF-7	Cell viability ROS generation	Pressure-induced amorphization	Pressure-induced amorphization reduced the toxicity of MOF.	[104]
ZIF-8	*In vivo*	Mice	Survival rate Body weight examination Histological examination	Pressure-induced amorphization	Pressure-induced amorphization reduced the toxicity of MOF.	[104]

blood mononuclear cells (PBMCs) compared to bare MIL-100. Meanwhile, both coated and uncoated MOFs induced almost no toxicity to human colorectal carcinoma cells (Caco-2). The IC_{80} value was estimated at 800 μg.mL^{-1}. Similar observations were made in the case of heparin-coated MIL-100, except that *in vitro* toxicity was measured against J774.A1 cells [74].

Recently, our group designed and synthesized UiO-66-NH_2 decorated with benzamide-like molecules based on *Citrus tangerine* leaf extract [75]. We found that the use of leaf extract is an ideal concept for modifying MOF-based nanocarriers as it increases cellular uptake, affects targeted drug release capability, and reduces aggregations in the specific tissues/organs. Based on the confocal laser scanning microscopy images, it was confirmed that drug (DOX) was simultaneously delivered to the cytoplasm of HT-29 and HeLa cancer cells and to the nucleus of HT-29. In addition, *in vivo* studies showed that MOF-based nanocarriers capped with leaf extract can also effectively target cancer cells located in the kidneys and liver. At the same time, it was demonstrated that cell viability against different cell lines (HEK-293, HeLa, HepG2, HT-29, MCF-7, PC12) was above 95% and 50% in the absence and presence of drug, respectively. Such low cytotoxicity results from the presence of constituents from the leaf extract, comprising many biomolecules that are completely safe for the living cells.

Several reports on the reduced toxicity of covalently modified MOFs can also be found in the literature. For example, poly(ethylene glycol) (PEG) which has been extensively studied by biomedical researchers [76–80] can enhance MOF hydrophilicity and water dispersibility, as well as improve drug release kinetics [81].

Interestingly, Lázaro *et al.* [82] suggested that PEG-functionalization of Zr-*fum* (Fig. 13a-b) aids in selective anticancer cytotoxicity in drug delivery (Fig. 13c). The results of their study, shown in Fig. 13d-e, demonstrates that drug (dichloroacetate, DCA)-loaded PEGylated Zr-*fum* causes severe toxicity to HeLa and MCF-7 cancer cells already at a concentration close to 0.5 mg.mL^{-1}, in contrast to unmodified or folic acid (FA)-modified Zr-*fum*, while no significant toxicity was induced to HeLa cells incubated with PEGylated Zr-*fum* without drug. In addition, PEGylated Zr-*fum* was well tolerated by J774 macrophage cells and peripheral blood lymphocytes (PBLs), regardless of the presence of the drug, as can be seen in Fig. 13f. It is assumed that this phenomenon results from partial internalization of PEGylated MOF through caveolae-mediated endocytosis. It is also worth mentioning that although PEGylated Zr-*fum* was the most internalized MOF, it did not induce ROS production in J774 cells as was the case with the control and FA-functionalized samples (Fig. 13g).

On the other hand, Xiao *et al.* [83] confirmed reduced *in vitro* and *in vivo* toxicity after FA modification of HKUST-1. For instance, modification with FA was shown to accelerate skin wound healing in diabetic mice. The time to 50% wound closure was 14 and 19 days after administration of FA-HKUST-1 and HKUST-1, respectively. Moreover, the authors investigated the toxicity of FA-modified Cu-based MOFs, such as NOT-100 and MOF-74, indicating that this strategy could also be applied to improve biocompatibility of other MOFs. Interestingly, Ji *et al.* [84] investigated the effect of HKUST-1 functionalization with FA on the reproductive system of mice. It was revealed that surface modification not only reduced the reproductive toxicity, but also improves pregnancy and foetus development of mice. For example, mice incubated with HKUST-1 indicated reduced expressions of 24 genes in the testes, including fertility-relative genes (e.g., Sycp1, Sycp2, Stag2, Sgol2a, Smc4, and Nipbl), DNA repair genes (e.g., Rock1, Rb1cc1), and cell death pathway genes (e.g., Rif1, Smc6) by 46–70% ($p < 0.01$) while FA-modified MOF showed no effect on gene expression.

Polysaccharides, such hyaluronic acid (HA), have been major components for biomedical research [79,85–101] and have been investigated for the surface modification of MOFs. Another promising approach to improving MOF cytocompatibility was proposed by Fu *et al.* [102]. They synthesized HA-modified ZIF-8-based chlorin e6 (Ce6) (ZIF-8@Ce6-HA) for photodynamic therapy. They found that HA surface modification prevented HepG2 cell death, whereas nearly 80% cells died with the non-coated ZIF-8@Ce6 (up to 3 μM). These results agreed with *in vivo* studies where, following ZIF-8@Ce6-HA treatment, no pathological changes were observed in various organs (liver, heart, spleen, lung, and kidney). However, non-coated ZIF-8@Ce6 induced hepatotoxicity as evidenced with a large number of vacuolated cells. Moreover, the irradiation of HepG2 treated with ZIF-8@Ce6-HA led to substantial cell death (88.4%), indicating an efficient therapeutic effect.

Other attempts have also been made to reduce MOF toxicity. For instance, Ma *et al.* [103] showed that the process of carbonization lowered the MOF-199 toxicity to white-rot fungus *Phanerochaete chrysosporium*. Unlike carbonized MOF-199, non-treated MOF-199 induced greater inhibition of fungal growth and enzyme activity, led to substantial fungal mycelium damage, and generated more oxidative stress.

Interesting study was also performed by Jiang *et al.* [104] who found that pressure-induced amorphization of ZIF-8 improved its *in vitro* and *in vivo* biocompatibility. The amorphization, achieved by inducing different amounts of pressure, was confirmed by XRD analysis (Fig. 14a). In addition, it was revealed that amorphous ZIF-8 (a-ZIF-8) particles became slightly larger and irregular, while its chemical structure remained the same (Fig. 14b-d).

The results of ECA-109 cell viability assay (Fig. 14e), showed significantly lower toxicity of ZIF-8 treated with a pressure of at least 0.6 MPa compared to its crystalline counterpart. This agreed with a reduction in Zn^{2+} release and ROS production, which are responsible for inducing toxicity in NPs. Similar observations were also made about the *in vivo* examination. For example, incubation with 100 mg.kg^{-1} of crystalline ZIF-8 resulted in the death of all mice, in contrast to a-ZIF-8 which did not affect the survival rate (Fig. 14f). Importantly, this trend was maintained when MOF filled with drug (5-Fu) was considered. As shown in Fig. 14g-i, the administration of 12 mg.kg^{-1} of a-ZIF-8 may successfully decrease the tumor volume, leading to the recovery of mice, without interfering with any organs, which would not be possible with untreated ZIF-8.

The attempts to reduce the toxicity of various MOFs so far and the main conclusions are briefly summarized in Table 2. In the light of the above findings, there are lots of opportunities to overcome the toxicity of MOFs. Importantly, several approaches were also found to be beneficial in terms of potential applications such as drug delivery due to increased cellular uptake and/or more efficient drug release. Since this study showed a great potential for MOF modification with various biomolecules, further investigation on the effect of other bio-based components such as polypeptides or nucleic acids on MOF performance should be conducted.

6. Path to clinical trials

The available literature together with this work demonstrates a great potential of various MOFs in biomedical applications, especially in drug delivery systems. The effectiveness of these structures in anti-tumor therapy has been repeatedly proven to exceed conventionally used solutions [59,105]. Although it may seem that such a treatment will soon be implemented in a real-world, still a long way should be paved to achieve this goal. A first step towards any biomedical applications is an in-depth evaluation of toxicity behavior under the influence of a chemical compound targeting specific cells/organs (*in vitro*) as well as the entire biological system (*in vivo*). This pre-clinical stage is extremely important because it provides a lot of valuable information about possible toxicity mechanisms and side effects. Importantly, considering the relevant conditions and various factors, it needs to be carried out in a thoughtful manner to minimize the subsequent risk to human health. Simultaneously, in addition to non-toxicity, the suitability of MOFs in the potential application must be justified. The performance properties including cellular uptake, chemical stability, release profile and others should be considered.

It can be concluded that so far only a few MOFs have been precisely

analyzed in terms of toxicity to confirm their biocompatibility while maintaining appropriate utility. For example, MIL-100(Fe) has been of a particular interest to the researchers in the field of MOF with more than 30 papers published on the subject. The recent advances and available data were collected and discussed in a review article [106]. The scientists summarized the toxicity profile, physicochemical stability of MIL-100(Fe) (considering various pH, temperature, and physiological conditions), as well as its application in biomedical sectors, including biosensors, phototherapy, and drug carriers. Although the results are promising, some aspects still need to be refined, such as the optimization of particle size or morphology control. However, in addition to scientific works, several biocompatible MOFs (their synthesis and application) have been patented recently. For example, Bin *et al.* [107] invented method for inhibiting tumor angiogenesis in mammals, comprising administering to a patient in need thereof an effective amount of a Fe-based MOF (MIL-101 or MIL-88B). According to the invention, MOF selectively inhibits the proliferation of cancer cells and vascular endothelial cell, while exhibiting low toxicity to normal cell. A particular efficacy was declared in the treatment of SKOV3 and HUVEC tumor cells. On the other hand, another patent [108] covers the chemo-radiation as an efficient method for tumor treatment involving the combination of radiotherapy and MOF-mediated drug delivery. The inventors discovered that intravenous administration of MOF (Hf-BDC) to mice provides synergistic enhancement of the therapeutic efficacy of radiotherapy which resulted in improved tumor growth inhibition and increased apoptosis without apparent toxicity or any side effects.

Although a lot of studies based on extensive publications and patents have been conducted to date, confirming the validity of MOFs for biomedical applications, there is still much to be done to go for clinical trials. To the best of our knowledge, the *in vivo* experiments on mammals are very limited. Even though MOFs were found to be successful in laboratory or in small animals, it does not mean that they would be safe and effective for humans. It is worth highlighting that clinical trials are not intended to assess toxicity, but to confirm the safety and effectiveness of a medical strategy. Because they are performed on humans, it comes with a huge responsibility. Therefore, only after a systematic and thorough research process, which almost guarantees safety, the clinical phase may begin. Nevertheless, there is always some risk as unpredictable side effects can occur that cannot be avoided (i.e., each organism has a different immune system and may react differently to the same substance). Although the process from scratch to clinical trials is very long and intricate, further research should not be discontinued even though the goal is not within reach. It is also worth mentioning that patience is still needed when treatment moves into the clinical phase. Although the process runs rather smoothly, it is time-consuming (usually takes from a few years to several decades). This is due, among others, to the need to sign many relevant regulatory and ethical approvals, to gather volunteers (from different countries, different age groups, etc.) or a long duration of treatment.

7. Conclusions and future directions

Metal-organic frameworks (MOFs) are a class of materials that have gained increasing attention in recent years due to their potential applications in various fields, including gas separation and storage, energy storage, catalysis, and biomedical applications. MOFs are hybrid materials composed of metal ions and organic linkers that form a porous and crystalline structure with high surface area and tunable properties. MOFs' unique properties make them promising candidates for developing novel therapeutics, such as drug delivery, medical imaging, and tissue engineering. However, the biocompatibility and toxicity of MOFs are essential considerations for their use in medical applications. Toxicity assessment of MOFs in biological environments is still a relatively new field of research. Nevertheless, the available *in vitro* and *in vivo* studies have revealed some crucial factors influencing MOF toxicity, such as their chemistry, particle size, morphology, and aggregation. MOFs have been shown to cause cellular damage, oxidative stress, inflammation, and genotoxicity *in vitro*, while *in vivo* studies have shown that they can cause organ damage and immune system dysregulation. The mechanisms of MOF toxicity are believed to be related to the release of metal ions from the MOF structures, as well as their size and surface properties.

To overcome inherent MOF toxicity, several strategies have been proposed such as surface modification, encapsulation, and the use of biodegradable MOFs. These approaches have shown promising results in reducing MOF toxicity while retaining their desirable properties. In addition, some researchers are exploring the use of MOFs for targeted drug delivery and medical imaging. These applications may offer a safer and more effective way of treating diseases and detecting medical conditions. One of the most promising applications of MOFs in medicine is drug delivery. MOFs' tunable properties and high surface area make them ideal candidates for carrying drugs and targeting specific cells or tissues. MOFs can encapsulate drugs, protecting them from degradation and improving their bioavailability. Furthermore, MOFs' unique properties, such as their pH responsiveness and stimuli-responsiveness, make them suitable for targeted drug delivery. MOFs can release drugs in response to specific triggers, such as pH changes or temperature changes, which can improve drug efficacy and reduce side effects. In addition, MOFs are being explored for medical imaging applications. MOFs' high surface area and porosity can be used to encapsulate imaging agents, such as contrast agents or radioactive isotopes. This can improve imaging sensitivity and specificity, enabling earlier disease detection and more accurate diagnosis. Furthermore, MOFs can be functionalized with targeting moieties, such as antibodies or peptides, to specifically bind to diseased cells or tissues, enabling precise imaging and diagnosis. Moreover, MOFs hold great potential in tissue engineering applications. MOFs' unique properties, such as their tunable porosity, surface chemistry, and biocompatibility, make them attractive candidates for developing scaffolds for tissue regeneration. MOFs can be functionalized with bioactive molecules, such as growth factors or extracellular matrix proteins, to promote cell adhesion, proliferation, and differentiation. Furthermore, MOFs can be used to deliver drugs or other therapeutic agents to the injured tissues, promoting tissue regeneration and repair.

Despite the promising applications of MOFs in medicine, several challenges need to be addressed before their clinical use. The first challenge is to establish standardized toxicity testing protocols and exposure limits. The toxicity of MOFs is highly dependent on their chemistry, size, and surface properties, making it challenging to develop a one-size-fits-all toxicity assessment. Therefore, it is essential to establish standardized protocols for toxicity testing and exposure limits to ensure the safety of MOFs in clinical applications. The second challenge is to identify suitable animal models for toxicity testing. MOF toxicity can vary significantly depending on the animal species, making it crucial to select appropriate animal models for toxicity studies. Moreover, the ethical implications of animals in research need to be considered. Alternatives testing such as *in vitro* assays and computational modelling, can be used to supplement animal studies and reduce the number of animals used in research. Another challenge is to develop scalable and cost-effective methods for MOF synthesis and functionalization. Most MOF synthesis methods are time-consuming and require high temperatures and pressures, which limit their scalability and reproducibility. In addition, functionalizing MOFs with bioactive molecules or targeting specific moieties can be challenging, requiring specialized expertise and equipment. Developing scalable and cost-effective methods for MOF synthesis and functionalization is essential to enable their widespread use for biomedical applications. What is missing as a prerequisite in this regard is a deeper understanding of the correlation between structural variables of MOFs (such as functionality, pore size, surface area, etc.) and their toxicity. This knowledge would help researchers avoid synthesizing unsafe MOFs for biomedical engineering applications.

Furthermore, the long-term biocompatibility and stability of MOFs *in vivo* need to be evaluated. MOFs' degradation and release of metal ions can cause toxicity and inflammation, making it crucial to evaluate them carefully. Long-term studies in animal models are needed to ensure MOF safety and efficacy and to identify any potential side effects. Despite these challenges, the potential of MOFs in medicine is vast, and further research is needed to realize their full potential. One promising direction for future research is to develop new MOFs with improved biocompatibility and targeting capabilities. By synthesizing MOFs with biodegradable linkers or designing MOFs that can resorb in response to specific triggers, it may be possible to improve their biocompatibility. However, it should be taken into account that despite the use of biocomponents, appropriate toxicity assessments must also be conducted to confirm the safety of MOFs. Moreover, by functionalizing MOFs with targeting moieties, such as antibodies or peptides, it may be possible to develop highly specific and effective drug delivery systems. Another promising direction for future research is to develop novel MOF-based theranostic platforms. Theranostics refers to the integration of diagnosis and therapy into a single platform, enabling personalized and precise medicine. By combining imaging and therapeutic capabilities into a single MOF-based platform, it may be possible to develop highly effective and targeted theranostic systems. For example, MOFs could be functionalized with imaging agents and therapeutic molecules and targeted to specific cells or tissues for imaging and treatment simultaneously.

Moreover, MOFs could be used to develop multifunctional scaffolds for tissue engineering applications. By incorporating bioactive molecules and drugs into MOF-based scaffolds, it may be possible to promote tissue regeneration and repair while simultaneously delivering therapeutic agents to the injured tissues. Furthermore, MOF-based scaffolds could be designed to release growth factors or other bioactive molecules in response to specific stimuli, such as changes in pH or temperature, enhancing their therapeutic potential.

In conclusion, MOFs are a promising class of materials with unique properties that make them attractive candidates for various medical applications, including drug delivery, medical imaging, and tissue engineering. However, their biocompatibility and toxicity need to be thoroughly evaluated before their clinical use. Several challenges need to be addressed, such as developing standardized toxicity testing protocols, identifying suitable animal models for preclinical trials, developing scalable and cost-effective methods for MOF synthesis and functionalization, and evaluating their long-term biocompatibility and stability *in vivo*. Nevertheless, the potential of MOFs in medicine is tremendous, and further research is needed to recognize and appreciate their full potential. By developing new MOFs with improved biocompatibility and targeting capabilities as well as designing novel MOF-based theranostic platforms and multifunctional scaffolds, the biomedical field will have a new platform to design highly effective and personalized medicine for various diseases and medical conditions.

Declaration of Competing Interest

The authors declare that they have no known competing financial interests or personal relationships that could have appeared to influence the work reported in this paper.

Data availability

No data was used for the research described in the article.

Acknowledgments

S.A.B. acknowledges the financial support from the National Institutes of Health (1R01EB027705) and the National Science Foundation (DMR 1847843).

References

[1] H. Furukawa, K.E. Cordova, M. O'Keeffe, O.M. Yaghi, The chemistry and applications of metal-organic frameworks, Science 341 (6149) (2013) 1230444.
[2] H.-C. Zhou, J.R. Long, O.M. Yaghi, Introduction to metal–organic frameworks, ACS Publications (2012) 673–674.
[3] M.R. Saeb, N. Rabiee, M. Mozafari, E. Mostafavi, Metal-organic frameworks (MOFs)-based nanomaterials for drug delivery, Materials 14 (13) (2021) 3652.
[4] M.R. Saeb, N. Rabiee, M. Mozafari, F. Verpoort, L.G. Voskressensky, R. Luque, Metal–organic frameworks (MOFs) for cancer therapy, Materials 14 (23) (2021) 7277.
[5] R. Ettlinger, U. Lächelt, R. Gref, P. Horcajada, T. Lammers, C. Serre, P. Couvreur, R.E. Morris, S. Wuttke, Toxicity of metal–organic framework nanoparticles: from essential analyses to potential applications, Chem. Soc. Rev. (2022).
[6] M. Carreon, S. Venna, Metal Organic Frameworks History and Structural Features, World Scientific Publishing Europe Ltd., Singapore, 2020, pp. 1–29.
[7] H. Li, M. Eddaoudi, M. O'Keeffe, O.M. Yaghi, Design and synthesis of an exceptionally stable and highly porous metal-organic framework, Nature 402 (6759) (1999) 276–279.
[8] S.M. Moosavi, A. Nandy, K.M. Jablonka, D. Ongari, J.P. Janet, P.G. Boyd, Y. Lee, B. Smit, H.J. Kulik, Understanding the diversity of the metal-organic framework ecosystem, Nat. Commun. 11 (1) (2020) 1–10.
[9] H.C. Fischer, W.C. Chan, Nanotoxicity: the growing need for in vivo study, Curr. Opin. Biotechnol. 18 (6) (2007) 565–571.
[10] A.K. Jain, D. Singh, K. Dubey, R. Maurya, S. Mittal, A.K. Pandey, Models and methods for in vitro toxicity, in: In vitro toxicology, Elsevier, 2018, pp. 45–65.
[11] M. Sajid, Toxicity of nanoscale metal organic frameworks: a perspective, Environ. Sci. Pollut. Res. 23 (15) (2016) 14805–14807.
[12] J. Liu, X. Zou, C. Liu, K. Cai, N. Zhao, W. Zheng, G. Zhu, Ionothermal synthesis and proton-conductive properties of NH 2-MIL-53 MOF nanomaterials, CrstEngComm 18 (4) (2016) 525–528.
[13] M. Kandiah, M.H. Nilsen, S. Usseglio, S. Jakobsen, U. Olsbye, M. Tilset, C. Larabi, E.A. Quadrelli, F. Bonino, K.P. Lillerud, Synthesis and stability of tagged UiO-66 Zr-MOFs, Chem. Mater. 22 (24) (2010) 6632–6640.
[14] J. Duan, Y. Sun, S. Chen, X. Chen, C. Zhao, A zero-dimensional nickel, iron–metal–organic framework (MOF) for synergistic N 2 electrofixation, J. Mater. Chem. A 8 (36) (2020) 18810–18815.
[15] X. He, V. Nguyen, Z. Jiang, D. Wang, Z. Zhu, W.-N. Wang, Highly-oriented one-dimensional MOF-semiconductor nanoarrays for efficient photodegradation of antibiotics, Cat. Sci. Technol. 8 (8) (2018) 2117–2123.
[16] C. Falaise, C. Volkringer, J.F. Vigier, N. Henry, A. Beaurain, T. Loiseau, Three-dimensional MOF-type architectures with tetravalent uranium hexanuclear motifs (U6O8), Chem.–A Eur. J. 19 (17) (2013) 5324–5331.
[17] M. Massoudinejad, M. Ghaderpoori, A. Shahsavani, A. Jafari, B. Kamarehie, A. Ghaderpoury, M.M. Amini, Ethylenediamine-functionalized cubic ZIF-8 for arsenic adsorption from aqueous solution: modeling, isotherms, kinetics and thermodynamics, J. Mol. Liq. 255 (2018) 263–268.
[18] Y. Wang, F. Wang, J. Zhang, Fast synthesis of hybrid zeolitic imidazolate frameworks (HZIFs) with exceptional acid–base stability from ZIF-8 precursors, Cryst. Growth Des. 19 (6) (2019) 3430–3434.
[19] H. Han, L. Kan, P. Li, G. Zhang, K. Li, W. Liao, Y. Liu, W. Chen, C.T. Hu, 4.8 nm Concave {M 72}(M= Co, Ni, Fe) metal-organic polyhedra capped by 18 calixarenes, Science China, Chemistry 64 (2021) 426–431.
[20] P. Deria, J.E. Mondloch, O. Karagiaridi, W. Bury, J.T. Hupp, O.K. Farha, Beyond post-synthesis modification: evolution of metal–organic frameworks via building block replacement, Chem. Soc. Rev. 43 (16) (2014) 5896–5912.
[21] P.Z. Moghadam, A. Li, X.-W. Liu, R. Bueno-Perez, S.-D. Wang, S.B. Wiggin, P. A. Wood, D. Fairen-Jimenez, Targeted classification of metal–organic frameworks in the Cambridge structural database (CSD), Chem. Sci. 11 (32) (2020) 8373–8387.
[22] X.-L. Chang, S.-T. Yang, G. Xing, Molecular toxicity of nanomaterials, J. Biomed. Nanotechnol. 10 (10) (2014) 2828–2851.
[23] S. Sharifi, S. Behzadi, S. Laurent, M.L. Forrest, P. Stroeve, M. Mahmoudi, Toxicity of nanomaterials, Chem. Soc. Rev. 41 (6) (2012) 2323–2343.
[24] Y.-C. Chen, K.-Y.-A. Lin, K.-F. Chen, X.-Y. Jiang, C.-H. Lin, In vitro renal toxicity evaluation of copper-based metal–organic framework HKUST-1 on human embryonic kidney cells, Environ. Pollut. 273 (2021), 116528.
[25] X. Yan, Q. Yang, X. Fang, P. Xiong, S. Liu, Z. Cao, C. Liao, S. Liu, G. Jiang, Co (ii)-based metal–organic framework induces apoptosis through activating the HIF-1α/BNIP3 signaling pathway in microglial cells, Environ. Sci. Nano 8 (10) (2021) 2866–2882.
[26] S.-T. Yang, J.-H. Liu, J. Wang, Y. Yuan, A. Cao, H. Wang, Y. Liu, Y. Zhao, Cytotoxicity of zinc oxide nanoparticles: importance of microenvironment, J. Nanosci. Nanotechnol. 10 (12) (2010) 8638–8645.
[27] Y. Li, S. Shang, J. Shang, W.-X. Wang, Toxicity assessment and underlying mechanisms of multiple metal organic frameworks using the green algae Chlamydomonas reinhardtii model, Environ. Pollut. 291 (2021), 118199.
[28] G. Crisponi, V.M. Nurchi, J.I. Lachowicz, M. Peana, S. Medici, M.A. Zoroddu, Toxicity of nanoparticles: etiology and mechanisms, in: Antimicrobial nanoarchitectonics, Elsevier, 2017, pp. 511–546.
[29] H.-J. Eom, J. Choi, Clathrin-mediated endocytosis is involved in uptake and toxicity of silica nanoparticles in Caenohabditis elegans, Chem. Biol. Interact. 311 (2019), 108774.
[30] R. Brayner, R. Ferrari-Iliou, N. Brivois, S. Djediat, M.F. Benedetti, F. Fiévet, Toxicological impact studies based on Escherichia coli bacteria in ultrafine ZnO nanoparticles colloidal medium, Nano Lett. 6 (4) (2006) 866–870.

[31] K.R. Raghupathi, R.T. Koodali, A.C. Manna, Size-dependent bacterial growth inhibition and mechanism of antibacterial activity of zinc oxide nanoparticles, Langmuir 27 (7) (2011) 4020–4028.
[32] P. Ruenraroengsak, P. Novak, D. Berhanu, A.J. Thorley, E. Valsami-Jones, J. Gorelik, Y.E. Korchev, T.D. Tetley, Respiratory epithelial cytotoxicity and membrane damage (holes) caused by amine-modified nanoparticles, Nanotoxicology 6 (1) (2012) 94–108.
[33] G. Gogniat, M. Thyssen, M. Denis, C. Pulgarin, S. Dukan, The bactericidal effect of TiO2 photocatalysis involves adsorption onto catalyst and the loss of membrane integrity, FEMS Microbiol. Lett. 258 (1) (2006) 18–24.
[34] P.K. Stoimenov, R.L. Klinger, G.L. Marchin, K.J. Klabunde, Metal oxide nanoparticles as bactericidal agents, Langmuir 18 (17) (2002) 6679–6686.
[35] Z.J. Deng, M. Liang, M. Monteiro, I. Toth, R.F. Minchin, Nanoparticle-induced unfolding of fibrinogen promotes Mac-1 receptor activation and inflammation, Nat. Nanotechnol. 6 (1) (2011) 39–44.
[36] F. Hao, Z.Y. Yan, X.P. Yan, Recent Advances in Research on the Effect of Physicochemical Properties on the Cytotoxicity of Metal-Organic Frameworks, Small Science 2 (9) (2022) 2200044.
[37] À. Ruyra, A. Yazdi, J. Espín, A. Carné-Sánchez, N. Roher, J. Lorenzo, I. Imaz, D. Maspoch, Synthesis, culture medium stability, and in vitro and in vivo zebrafish embryo toxicity of metal–organic framework nanoparticles, Chem.–A Eur. J. 21 (6) (2015) 2508–2518.
[38] F. Hao, X.-P. Yan, Nano-sized zeolite-like metal-organic frameworks induced hematological effects on red blood cell, J. Hazard. Mater. 424 (2022), 127353.
[39] X. Zhang, X. Hu, H. Wu, L. Mu, Persistence and Recovery of ZIF-8 and ZIF-67 Phytotoxicity, Environ. Sci. Tech. 55 (22) (2021) 15301–15312.
[40] R. Grall, T. Hidalgo, J. Delic, A. Garcia-Marquez, S. Chevillard, P. Horcajada, In vitro biocompatibility of mesoporous metal (III; Fe, Al, Cr) trimesate MOF nanocarriers, J. Mater. Chem. B 3 (42) (2015) 8279–8292.
[41] T. Hidalgo, R. Simón-Vázquez, A. González-Fernández, P. Horcajada, Cracking the immune fingerprint of metal–organic frameworks, Chem. Sci. 13 (4) (2022) 934–944.
[42] S. Wuttke, A. Zimpel, T. Bein, S. Braig, K. Stoiber, A. Vollmar, D. Müller, K. Haastert-Talini, J. Schaeske, M. Stiesch, Validating Metal-Organic Framework Nanoparticles for Their Nanosafety in Diverse Biomedical Applications, Adv. Healthc. Mater. 6 (2) (2017) 1600818.
[43] W. Duan, S. Qiao, M. Zhuo, J. Sun, M. Guo, F. Xu, J. Liu, T. Wang, X. Guo, Y. Zhang, Multifunctional platforms: metal-organic frameworks for cutaneous and cosmetic treatment, Chem 7 (2) (2021) 450–462.
[44] I. Sifaoui, I. Pacheco-Fernández, J.E. Piñero, V. Pino, J. Lorenzo-Morales, A Simple in vivo Assay Using Amphipods for the Evaluation of Potential Biocompatible Metal-Organic Frameworks, Front. Bioeng. Biotechnol. 9 (2021), 584115.
[45] C. Tamames-Tabar, D. Cunha, E. Imbuluzqueta, F. Ragon, C. Serre, M.J. Blanco-Prieto, P. Horcajada, Cytotoxicity of nanoscaled metal–organic frameworks, J. Mater. Chem. B 2 (3) (2014) 262–271.
[46] T. Baati, L. Njim, F. Neffati, A. Kerkeni, M. Bouttemi, R. Gref, M.F. Najjar, A. Zakhama, P. Couvreur, C. Serre, In depth analysis of the in vivo toxicity of nanoparticles of porous iron (III) metal–organic frameworks, Chem. Sci. 4 (4) (2013) 1597–1607.
[47] C.I. Yen, S.M. Liu, W.S. Lo, J.W. Wu, Y.H. Liu, R.J. Chein, R. Yang, K.C.W. Wu, J. R. Hwu, N. Ma, Cytotoxicity of postmodified zeolitic imidazolate Framework-90 (ZIF-90) nanocrystals: correlation between functionality and toxicity, Chem.–A Eur. J. 22 (9) (2016) 2925–2929.
[48] N. Rabiee, M. Atarod, M. Tavakolizadeh, S. Asgari, M. Rezaei, O. Akhavan, A. Pourjavadi, M. Jouyandeh, E.C. Lima, A.H. Mashhadzadeh, Green metal-organic frameworks (MOFs) for biomedical applications, Microporous Mesoporous Mater. 335 (2022), 111670.
[49] N. Rabiee, M. Bagherzadeh, M. Jouyandeh, P. Zarrintaj, M.R. Saeb, M. Mozafari, M. Shokouhimehr, R.S. Varma, Natural polymers decorated MOF-MXene nanocarriers for co-delivery of doxorubicin/pCRISPR, ACS Appl. Bio Mater. 4 (6) (2021) 5106–5121.
[50] S. Ahmadi, V. Jajarmi, M. Ashrafizadeh, A. Zarrabi, J.T. Haponiuk, M.R. Saeb, E. C. Lima, M. Rabiee, N. Rabiee, Mission impossible for cellular internalization: When porphyrin alliance with UiO-66-NH2 MOF gives the cell lines a ride, J. Hazard. Mater. 436 (2022), 129259.
[51] T. Simon-Yarza, A. Mielcarek, P. Couvreur, C. Serre, Nanoparticles of metal-organic frameworks: on the road to in vivo efficacy in biomedicine, Adv. Mater. 30 (37) (2018) 1707365.
[52] D. Ramakrishna, P. Rao, Nanoparticles: is toxicity a concern? EJIFCC 22 (4) (2011) 92.
[53] Z. Zhu, S. Jiang, Y. Liu, X. Gao, S. Hu, X. Zhang, C. Huang, Q. Wan, J. Wang, X. Pei, Micro or nano: Evaluation of biosafety and biopotency of magnesium metal organic framework-74 with different particle sizes, Nano Res. 13 (2) (2020) 511–526.
[54] S. Jiang, J. Wang, Z. Zhu, S. Shan, Y. Mao, X. Zhang, X. Pei, C. Huang, Q. Wan, The synthesis of nano bio-MOF-1 with a systematic evaluation on the biosafety and biocompatibility, Microporous Mesoporous Mater. 334 (2022), 111773.
[55] P. Chen, M. He, B. Chen, B. Hu, Size-and dose-dependent cytotoxicity of ZIF-8 based on single cell analysis, Ecotoxicol. Environ. Saf. 205 (2020), 111110.
[56] D. Wang, L. Bai, X. Huang, W. Yan, S. Li, Size-dependent acute toxicity and oxidative damage caused by cobalt-based framework (ZIF-67) to Photobacterium phosphoreum, Sci. Total Environ. 851 (2022), 158317.
[57] S. Deng, X. Yan, P. Xiong, G. Li, T. Ku, N. Liu, C. Liao, G. Jiang, Nanoscale cobalt-based metal-organic framework impairs learning and memory ability without noticeable general toxicity: First in vivo evidence, Sci. Total Environ. 771 (2021), 145063.
[58] F. Hao, Z.-Y. Yan, X.-P. Yan, Size-and shape-dependent cytotoxicity of nano-sized Zr-based porphyrinic metal-organic frameworks to macrophages, Sci. Total Environ. 833 (2022), 155309.
[59] D. Duan, H. Liu, M. Xu, M. Chen, Y. Han, Y. Shi, Z. Liu, Size-controlled synthesis of drug-loaded zeolitic imidazolate framework in aqueous solution and size effect on their cancer theranostics in vivo, ACS Appl. Mater. Interfaces 10 (49) (2018) 42165–42174.
[60] Y.Y. Liu, L.J. Chen, X. Zhao, X.P. Yan, Effect of Topology on Photodynamic Sterilization of Porphyrinic Metal-Organic Frameworks, Chemistry–A, European Journal 27 (39) (2021) 10151–10159.
[61] J. Zhou, Y. Li, L. Wang, Z. Xie, Structural diversity of nanoscale zirconium porphyrin MOFs and their photoactivities and biological performances, J. Mater. Chem. B 9 (37) (2021) 7760–7770.
[62] E. Joseph, G. Singhvi, Multifunctional nanocrystals for cancer therapy: a potential nanocarrier, Nanomater. Drug Delivery Therapy (2019) 91–116.
[63] J.M. Berg, A. Romoser, N. Banerjee, R. Zebda, C.M. Sayes, The relationship between pH and zeta potential of~ 30 nm metal oxide nanoparticle suspensions relevant to in vitro toxicological evaluations, Nanotoxicology 3 (4) (2009) 276–283.
[64] A. Zimpel, N. Al Danaf, B. Steinborn, J. Kuhn, M. Höhn, T. Bauer, P. Hirschle, W. Schrimpf, H. Engelke, E. Wagner, Coordinative binding of polymers to metal–organic framework nanoparticles for control of interactions at the biointerface, ACS Nano 13 (4) (2019) 3884–3895.
[65] N. Rabiee, M. Atarod, M. Tavakolizadeh, S. Asgari, M. Rezaei, O. Akhavan, A. Pourjavadi, M. Jouyandeh, E.C. Lima, A.H. Mashhadzadeh, Green metal-organic frameworks (MOFs) for biomedical applications, Microporous Mesoporous Mater. 111670 (2022).
[66] E.S. Grape, J.G. Flores, T. Hidalgo, E. Martínez-Ahumada, A. Gutiérrez-Alejandre, A. Hautier, D.R. Williams, M. O'Keeffe, L. Öhrström, T. Willhammar, A robust and biocompatible bismuth ellagate MOF synthesized under green ambient conditions, J. Am. Chem. Soc. 142 (39) (2020) 16795–16804.
[67] M.P. Abuçafy, B.L. Caetano, B.G. Chiari-Andréo, B. Fonseca-Santos, A.M. do Santos, M. Chorilli, L.A. Chiavacci, Supramolecular cyclodextrin-based metal-organic frameworks as efficient carrier for anti-inflammatory drugs, Eur. J. Pharm. Biopharm. 127 (2018) 112–119.
[68] V. Agostoni, P. Horcajada, V. Rodriguez-Ruiz, H. Willaime, P. Couvreur, C. Serre, R. Gref, 'Green' fluorine-free mesoporous iron (III) trimesate nanoparticles for drug delivery, Green Mater. 1 (4) (2013) 209–217.
[69] S. Li, L. Tan, X. Meng, Nanoscale metal-organic frameworks: synthesis, biocompatibility, imaging applications, and thermal and dynamic therapy of tumors, Adv. Funct. Mater. 30 (13) (2020) 1908924.
[70] E. Ploetz, A. Zimpel, V. Cauda, D. Bauer, D.C. Lamb, C. Haisch, S. Zahler, A. M. Vollmar, S. Wuttke, H. Engelke, Metal–organic framework nanoparticles induce pyroptosis in cells controlled by the extracellular pH, Adv. Mater. 32 (19) (2020) 1907267.
[71] S. Wuttke, S. Braig, T. Preiß, A. Zimpel, J. Sicklinger, C. Bellomo, J.O. Rädler, A. M. Vollmar, T. Bein, MOF nanoparticles coated by lipid bilayers and their uptake by cancer cells, Chem. Commun. 51 (87) (2015) 15752–15755.
[72] J. Yang, X. Chen, Y. Li, Q. Zhuang, P. Liu, J. Gu, Zr-based MOFs shielded with phospholipid bilayers: improved biostability and cell uptake for biological applications, Chem. Mater. 29 (10) (2017) 4580–4589.
[73] T. Hidalgo, M. Giménez-Marqués, E. Bellido, J. Avila, M. Asensio, F. Salles, M. Lozano, M. Guillevic, R. Simón-Vázquez, A. González-Fernández, Chitosan-coated mesoporous MIL-100 (Fe) nanoparticles as improved bio-compatible oral nanocarriers, Sci. Rep. 7 (1) (2017) 1–14.
[74] E. Bellido, T. Hidalgo, M.V. Lozano, M. Guillevic, R. Simón-Vázquez, M. J. Santander-Ortega, Á. González-Fernández, C. Serre, M.J. Alonso, P. Horcajada, Heparin-engineered mesoporous iron metal-organic framework nanoparticles: toward stealth drug nanocarriers, Adv. Healthc. Mater. 4 (8) (2015) 1246–1257.
[75] N. Rabiee, A.M. Ghadiri, V. Alinezhad, A. Sedaghat, S. Ahmadi, Y. Fatahi, P. Makvandi, M.R. Saeb, M. Bagherzadeh, M. Asadnia, Synthesis of green benzamide-decorated UiO-66-NH2 for biomedical applications, Chemosphere 299 (2022), 134359.
[76] S.A. Benchérif, A. Srinivasan, J.A. Sheehan, L.M. Walker, C. Gayathri, R. Gil, J. O. Hollinger, K. Matyjaszewski, N.R. Washburn, End-group effects on the properties of PEG-co-PGA hydrogels, Acta Biomater. 5 (6) (2009) 1872–1883.
[77] S.A. Benchérif, J.A. Sheehan, J.O. Hollinger, L.M. Walker, K. Matyjaszewski, N. R. Washburn, Influence of cross-linker chemistry on release kinetics of PEG-co-PGA hydrogels, Journal of Biomedical Materials Research Part A: An Official Journal of The Society for Biomaterials, The Japanese Society for Biomaterials, and The Australian Society for Biomaterials and the Korean Society for, Biomaterials 90 (1) (2009) 142–153.
[78] S.A. Benchérif, H. Gao, A. Srinivasan, D.J. Siegwart, J.O. Hollinger, N. R. Washburn, K. Matyjaszewski, Cell-adhesive star polymers prepared by ATRP, Biomacromolecules 10 (7) (2009) 1795–1803.
[79] M.H. Bhuiyan, A.N. Clarkson, M.A. Ali, Optimization of thermoresponsive chitosan/β-glycerophosphate hydrogels for injectable neural tissue engineering application, Colloids Surf. B Biointerfaces 224 (2023), 113193.
[80] J.A. Yoon, S.A. Benchérif, B. Aksak, E.K. Kim, T. Kowalewski, J.K. Oh, K. Matyjaszewski, Thermoresponsive hydrogel scaffolds with tailored hydrophilic pores, Chem.–Asian J. 6 (1) (2011) 128–136.
[81] S. Beg, M. Rahman, A. Jain, S. Saini, P. Midoux, C. Pichon, F.J. Ahmad, S. Akhter, Nanoporous metal organic frameworks as hybrid polymer–metal composites for

drug delivery and biomedical applications, Drug Discov. Today 22 (4) (2017) 625–637.
[82] I. Abánades Lázaro, S. Haddad, J.M. Rodrigo-Munoz, R.J. Marshall, B. Sastre, V. Del Pozo, D. Fairen-Jimenez, R.S. Forgan, Surface-functionalization of Zr-fumarate MOF for selective cytotoxicity and immune system compatibility in nanoscale drug delivery, ACS Appl. Mater. Interfaces 10 (37) (2018) 31146–31157.
[83] J. Xiao, Y. Zhu, S. Huddleston, P. Li, B. Xiao, O.K. Farha, G.A. Ameer, Copper metal–organic framework nanoparticles stabilized with folic acid improve wound healing in diabetes, ACS Nano 12 (2) (2018) 1023–1032.
[84] X. Ji, Y. Mo, H. Li, W. Zhao, A. Zhong, S. Li, Q. Wang, X. Duan, J. Xiao, Gender-dependent reproductive toxicity of copper metal–organic frameworks and attenuation by surface modification, Nanoscale 13 (15) (2021) 7389–7402.
[85] T. Abdullah, T. Colombani, T. Alade, S.A. Bencherif, A. Memic, Injectable lignin-co-gelatin cryogels with antioxidant and antibacterial properties for biomedical applications, Biomacromolecules 22 (10) (2021) 4110–4121.
[86] L. Boulais, R. Jellali, U. Pereira, E. Leclerc, S.A. Bencherif, C. Legallais, Cryogel-integrated biochip for liver tissue engineering, ACS Appl. Bio Mater. 4 (7) (2021) 5617–5626.
[87] K. Mortezaee, J. Majidpoor, Cellular immune states in SARS-CoV-2-induced disease, Front. Immunol. 13 (2022).
[88] K. Joshi Navare, T. Colombani, M. Rezaeeyazdi, N. Bassous, D. Rana, T. Webster, A. Memic, S.A. Bencherif, Needle-injectable microcomposite cryogel scaffolds with antimicrobial properties, Sci. Rep. 10 (1) (2020) 1–16.
[89] O. Gsib, L.J. Eggermont, C. Egles, S.A. Bencherif, Engineering a macroporous fibrin-based sequential interpenetrating polymer network for dermal tissue engineering, Biomater. Sci. 8 (24) (2020) 7106–7116.
[90] A. Memic, M. Rezaeeyazdi, P. Villard, Z.J. Rogers, T. Abudula, T. Colombani, S. A. Bencherif, Effect of polymer concentration on autoclaved cryogel properties, Macromol. Mater. Eng. 305 (5) (2020) 1900824.
[91] P. Villard, M. Rezaeeyazdi, T. Colombani, K. Joshi-Navare, D. Rana, A. Memic, S. A. Bencherif, Autoclavable and injectable cryogels for biomedical applications, Adv. Healthc. Mater. 8 (17) (2019) 1900679.
[92] D. Rana, T. Colombani, B. Saleh, H.S. Mohammed, N. Annabi, S.A. Bencherif, Engineering injectable, biocompatible, and highly elastic bioadhesive cryogels, Materials Today Bio 19 (2023), 100572.
[93] J. Kim, S.A. Bencherif, W.A. Li, D.J. Mooney, Cell-Friendly Inverse Opal-Like Hydrogels for a Spatially Separated Co-Culture System, Macromol. Rapid Commun. 35 (18) (2014) 1578–1586.
[94] M. Rezaeeyazdi, T. Colombani, L.J. Eggermont, S.A. Bencherif, Engineering hyaluronic acid-based cryogels for CD44-mediated breast tumor reconstruction, Materials Today Bio 13 (2022), 100207.
[95] T. Colombani, L.J. Eggermont, Z.J. Rogers, L.G. McKay, L.E. Avena, R.I. Johnson, N. Storm, A. Griffiths, S.A. Bencherif, Biomaterials and Oxygen Join Forces to Shape the Immune Response and Boost COVID-19 Vaccines, Adv. Sci. 8 (18) (2021) 2100316.
[96] T. He, B. Li, T. Colombani, K. Joshi-Navare, S. Mehta, J. Kisiday, S.A. Bencherif, A.G. Bajpayee, Hyaluronic acid-based shape-memory cryogel scaffolds for focal cartilage defect repair, Tissue Eng. A 27 (11–12) (2021) 748–760.
[97] T. Colombani, Z.J. Rogers, L.J. Eggermont, S.A. Bencherif, Harnessing biomaterials for therapeutic strategies against COVID-19, Emergent Mater. 4 (2021) 9–18.
[98] J.E. Prata, T.A. Barth, S.A. Bencherif, N.R. Washburn, Complex fluids based on methacrylated hyaluronic acid, Biomacromolecules 11 (3) (2010) 769–775.
[99] S. Mahdavi, A. Amirsadeghi, A. Jafari, S.V. Niknezhad, S.A. Bencherif, Avian egg: a multifaceted biomaterial for tissue engineering, Ind. Eng. Chem. Res. 60 (48) (2021) 17348–17364.
[100] T. Abdullah, K. Bhatt, L.J. Eggermont, N. O'Hare, A. Memic, S.A. Bencherif, Supramolecular self-assembled peptide-based vaccines: current state and future perspectives, Front. Chem. 8 (2020), 598160.
[101] Z.J. Rogers, M.P. Zeevi, R. Koppes, S.A. Bencherif, Electroconductive hydrogels for tissue engineering: current status and future perspectives, Bioelectricity 2 (3) (2020) 279–292.
[102] X. Fu, Z. Yang, T. Deng, J. Chen, Y. Wen, X. Fu, L. Zhou, Z. Zhu, C. Yu, A natural polysaccharide mediated MOF-based Ce6 delivery system with improved biological properties for photodynamic therapy, J. Mater. Chem. B 8 (7) (2020) 1481–1488.
[103] Q. Ma, Q. Zhang, T. Maimaiti, S. Lan, X. Liu, Y. Wang, Q. Li, H. Luo, B. Yu, S.-T. Yang, Carbonization reduces the toxicity of metal-organic framework MOF-199 to white-rot fungus Phanerochaete chrysosporium, J. Environ. Chem. Eng. 9 (6) (2021), 106705.
[104] Z. Jiang, Y. Li, Z. Wei, B. Yuan, Y. Wang, O.U. Akakuru, Y. Li, J. Li, A. Wu, Pressure-induced amorphous zeolitic imidazole frameworks with reduced toxicity and increased tumor accumulation improves therapeutic efficacy In vivo, Bioact. Mater. 6 (3) (2021) 740–748.
[105] J. Bi, Y. Zheng, L. Fang, Y. Guan, A. Ma, J. Wu, Nano-sized MIL-100 (Fe) as a carrier material for nitidine chloride reduces toxicity and enhances anticancer effects in vitro, J. Inorg. Organomet. Polym Mater. 30 (2020) 3388–3395.
[106] C.R. Quijia, C. Lima, C. Silva, R.C. Alves, R. Frem, M. Chorilli, Application of MIL-100 (Fe) in drug delivery and biomedicine, J. Drug Delivery Sci. Technol. 61 (2021), 102217.
[107] B. Li, D. Chen, J. Wang, M. Nie, Use of metal-organic framework as tumor angiogenesis inhibitor, Google Patents, 2020.
[108] C.G.C. Sun, M.J. Neufeld, A.N. DuRoss, Nanoscale metal-organic frameworks for enhanced tumor chemoradiation, Google Patents (2021).